Ecological Modelling 359 (2017) 201–219

Contents lists available at ScienceDirect

Ecological Modelling

journal homepage: www.elsevier.com/locate/ecolmodel

Quantifying indirect groundwater-mediated effects of urbanization on agroecosystem productivity using MODFLOW-AgroIBIS (MAGI), a complete critical zone model

Samuel C. Zipper[a,*,1,2], Mehmet Evren Soylu[b,c], Christopher J. Kucharik[c,d,3], Steven P. Loheide II[a,1]

[a] Department of Civil & Environmental Engineering, University of Wisconsin-Madison, Madison, WI, USA
[b] Ankara, Turkey
[c] Nelson Institute Center for Sustainability and the Global Environment, University of Wisconsin-Madison, Madison, WI, USA
[d] Department of Agronomy, University of Wisconsin-Madison, Madison, WI, USA

ARTICLE INFO

Article history:
Received 21 January 2017
Received in revised form 4 May 2017
Accepted 5 June 2017

Keywords:
Land use change
Groundwater recharge
Urbanization
Agroecosystem modeling
Dynamic vegetation models
Groundwater-land surface coupling

ABSTRACT

Sustainably accommodating future population growth and meeting global food requirements requires understanding feedbacks between ecosystems and belowground hydrological processes. Here, we introduce MODFLOW-AgroIBIS (MAGI), a new dynamic ecosystem model including groundwater flow, and use MAGI to explore the indirect impacts of land use change (urbanization) on landscape-scale agroecosystem productivity (corn yield). We quantify the degree to which urbanization can indirectly impact yield in surrounding areas by changing the amount of groundwater recharge locally and the water table dynamics at landscape scales. We find that urbanization can cause increases or decreases in yield elsewhere, with changes up to approximately +/− 40% under the conditions simulated due entirely to altered groundwater-land surface interactions. Our results indicate that land use change in upland areas has the largest impact on water table depth over the landscape. However, there is a spatial mismatch between areas with the largest water table response to urbanization elsewhere (upland areas) and locations with the strongest yield response to urbanization elsewhere (midslope areas). This mismatch arises from differences in baseline water table depth prior to urbanization. Yield response to urbanization in lowland areas is relatively localized despite large changes to the vertical water balance due to stabilizing ecohydrological feedbacks between root water uptake and lateral groundwater flow. These results demonstrate that hydrological impacts of land use change can propagate through subsurface flow to indirectly impact surrounding ecosystems, and these subsurface connections should be considered when planning land use at a landscape scale to avoid negative outcomes associated with land use change.

1. Introduction

Land use/land cover (LULC) change is a primary driver of global change with diverse impacts on ecosystems, including altering freshwater availability, reducing biosphere integrity, changing biochemical flows, increasing atmospheric aerosol loading, and contributing to climate change (Foley, 2005; Foley et al., 2011; Steffen et al., 2015; Turner et al., 2007). In particular, LULC change can have diverse impacts on the hydrological cycle, often facilitated by changes in ecological processes. During urbanization, for instance, the interplay between vegetation and impervious areas influence the degree to which runoff, groundwater recharge, and evapotranspiration (ET) are affected (Bhaskar et al., 2015, 2016; Cho et al., 2009; Fry and Maxwell, 2017; Newcomer et al., 2014; Shields and Tague, 2015; Zipper et al., 2016b, 2017). Ecohydrological processes play a similar role in other LULC change pathways; conversion from perennial ecosystems to row-crop agriculture, for example, is often associated with a reduction in growing season length and evapotranspiration (ET) due to changes in terrestrial ecosystem processes, which can lead to an increase in groundwa-

* Corresponding author.
E-mail addresses: szipper@wisc.edu (S.C. Zipper), evrensoylu@gmail.com (M.E. Soylu), kucharik@wisc.edu (C.J. Kucharik), loheide@wisc.edu (S.P. Loheide II).
[1] Department of Civil & Environmental Engineering, University of Wisconsin-Madison, 1415 Engineering Dr, 53706, Madison, WI, USA.
[2] Present address: Department of Earth & Planetary Sciences, McGill University, Montreal QC
[3] Department of Agronomy, University of Wisconsin-Madison, 1575 Linden Dr, Madison, WI, 53706, USA.

http://dx.doi.org/10.1016/j.ecolmodel.2017.06.002
0304-3800/

ter recharge (Amdan et al., 2013; Giménez et al., 2016; Kim and Jackson, 2012; Scanlon et al., 2005; Yira et al., 2016).

Understanding the impacts of LULC on interactions between shallow groundwater and ecological processes is a particularly important question, as shallow groundwater is within 3 m of the land surface in an estimated 7–17% of global land area (Fan et al., 2013). LULC change impacts groundwater flow by altering groundwater recharge and discharge in ways that are both complex and hard to quantify (Bhaskar et al., 2015; Bhaskar and Welty, 2015; Oliveira et al., 2017; Passarello et al., 2012; Robertson and Sharp, 2015; Silveira et al., 2016). Furthermore, groundwater can exert a major control over energy and water balances at the land surface by altering near-surface soil moisture (Hain et al., 2015; Houspanossian et al., 2016; Kollet and Maxwell, 2008; Maxwell and Condon, 2016; Maxwell and Kollet, 2008; Miguez-Macho and Fan, 2012; Soylu et al., 2011). The altered water availability can have both positive and negative effects on the productivity and composition of both natural and managed ecosystems (Booth and Loheide, 2012; Florio et al., 2014; Lowry et al., 2011; Lowry and Loheide, 2010; Nosetto et al., 2009). Of particular note in the face of growing global food demand are the impacts of shallow groundwater on agricultural productivity. Shallow groundwater can increase yield during drought by providing a supplemental water supply ('groundwater yield subsidy') or decrease yield during wet conditions by enhancing oxygen stress ('groundwater yield penalty') (Zipper et al., 2015). Increasing groundwater recharge due to LULC change has been associated with a variety of negative impacts on ecosystems, including increased risk of flooding (Booth et al., 2016; Kuppel et al., 2015; Nosetto et al., 2015) and groundwater salinization due to the mobilization of unsaturated zone salts (George et al., 1999; Nosetto et al., 2013).

While interactions between shallow groundwater and ecosystems are often explored from a one-dimensional perspective (e.g. Ghamarnia et al., 2010; Huo et al., 2012a, 2012b; Karimi et al., 2011; Luo and Sophocleous, 2010), LULC mosaics can induce heterogeneous recharge and discharge patterns at local scales, particularly where perennial and annual ecosystems are in close proximity (Giménez et al., 2016; Nosetto et al., 2012). This heterogeneity can lead to surprising effects in the lateral dimension; Bhaskar et al. (2016), for example, noted that exurban development in headwater areas could lead to streamflow deficits downstream by drawing down groundwater, though modeled impacts surrounding Baltimore were primarily local. Similarly, Condon and Maxwell (2014) found that the largest drawdown due to groundwater irrigation in the Little Washita Basin (Oklahoma, USA) was not in the lowlands where the majority of irrigation was located, but rather in the uplands due to divergence of groundwater flow from topographically high areas. Recent work has highlighted the importance of considering impacts of lateral groundwater flow on land surface processes such as runoff generation and ET (Fan, 2015; Maxwell and Condon, 2016; Maxwell and Kollet, 2008).

Despite these recent advances, the degree to which LULC decisions in one location may indirectly impact ecological processes in surrounding areas by altering groundwater recharge and subsurface flow remains poorly understood, in large part due to limitations in the capabilities of current modeling approaches. Existing models typically specialize in the simulation of either water or vegetation dynamics, rather than both. Widely used soil hydrology models including HYDRUS (Šimůnek et al., 2013), COMSOL (Booth and Loheide, 2010, 2012), and unsaturated zone packages for MODFLOW (Niswonger et al., 2006; Thoms et al., 2006; Twarakavi et al., 2008) either oversimplify or do not explicitly represent vegetation. In contrast, existing land surface and agroecosystem models such as LPJmL (Bondeau et al., 2007; Sitch et al., 2003), DSSAT (Jones et al., 2003), and APSIM (McCown et al., 1996; Wang et al., 2002) capture vegetation dynamics well, but represent below-ground soil hydrology in a simplified manner. The ParFlow-based family of models, including ParFlow.CLM (Maxwell and Miller, 2005) and TerrSysMP (Gasper et al., 2014; Shrestha et al., 2014), represents the current state of the art. ParFlow.CLM consists of ParFlow, a fully three-dimensional surface/subsurface hydrological flow model designed for parallelized computing, coupled with the Community Land Model (Dai et al., 2003), a land surface model originally developed for interfacing with climate models. While powerful and widely used in the scientific community, the representation of vegetation, particularly agroecosystems, in CLM remains limited. Certain weaknesses, including lack of differentiation between different agricultural plant functional types (Sulis et al., 2014), a requirement to provide phenological parameters such as leaf area index (LAI) as input data rather than simulating the explicit growth of plants, an inability to provide quantitative yield estimates (Drewniak et al., 2013), and a lack of nutrient cycling limit the ability of ParFlow.CLM to answer certain questions related to LULC change and agricultural management impacts on ecological processes and the hydrological cycle.

In this study, we introduce MODFLOW-AgroIBIS (MAGI), a new modeling framework capable of dynamically simulating vegetation growth and nutrient cycling (nitrogen and phosphorus) in response to environmental conditions while employing a physically-based approach to quantify the movement of water and energy across the groundwater-unsaturated zone-vegetation continuum (also known as the critical zone). MAGI uses the latest version of AgroIBIS (Soylu et al., 2014; Zipper et al., 2015; Motew et al., 2017), which has soil physics adapted from HYDRUS-1D, as a land surface and unsaturated zone module for MODFLOW-2005, a widely used groundwater flow model (Harbaugh, 2005). This coupled approach gives MAGI the advantages of each of three widely-used and well-validated models: (1) AgroIBIS, a process-based ecosystem model including dynamic vegetation growth in both natural and managed ecosystems (Kucharik et al., 2000; Kucharik and Brye, 2003); (2) HYDRUS-1D, a variably saturated flow model using the Richards Equation to represent water and heat transport (Šimůnek et al., 2013); and (3) MODFLOW-2005, a modular groundwater flow model (Harbaugh, 2005).

After describing and validating the new model (Sections 2 and 3, respectively), we then use MAGI to address the following questions:

(1) Can changes in LULC (urbanization) in one location lead to changes in agroecosystem productivity (corn yield) in surrounding areas by altering groundwater flow and root zone water availability?
(2) Where on the landscape is agroecosystem productivity most sensitive to urbanization elsewhere?
(3) Where on the landscape does urbanization exert the strongest influence on agroecosystem productivity elsewhere?

2. Model description

2.1. AgroIBIS

AgroIBIS is a one-dimension (vertical) process-based ecosystem model that can simulate both managed and natural ecosystem dynamics with coupled water, energy, carbon, nitrogen, and phosphorus cycles; a schematic overview of some of the major processes included in AgroIBIS is shown in Fig. 1a. AgroIBIS was developed in the early 2000s to extend the capability of the Integrated BIosphere Simulator (IBIS; Foley et al., 1996) global dynamic vegetation model to simulate agroecosystems, at which time agricultural outputs such as grain yield, harvest index, plant nitrogen concentrations, season leaf area index (LAI) patterns, and the land surface energy balance were validated (Donner and Kucharik, 2003; Kucharik and

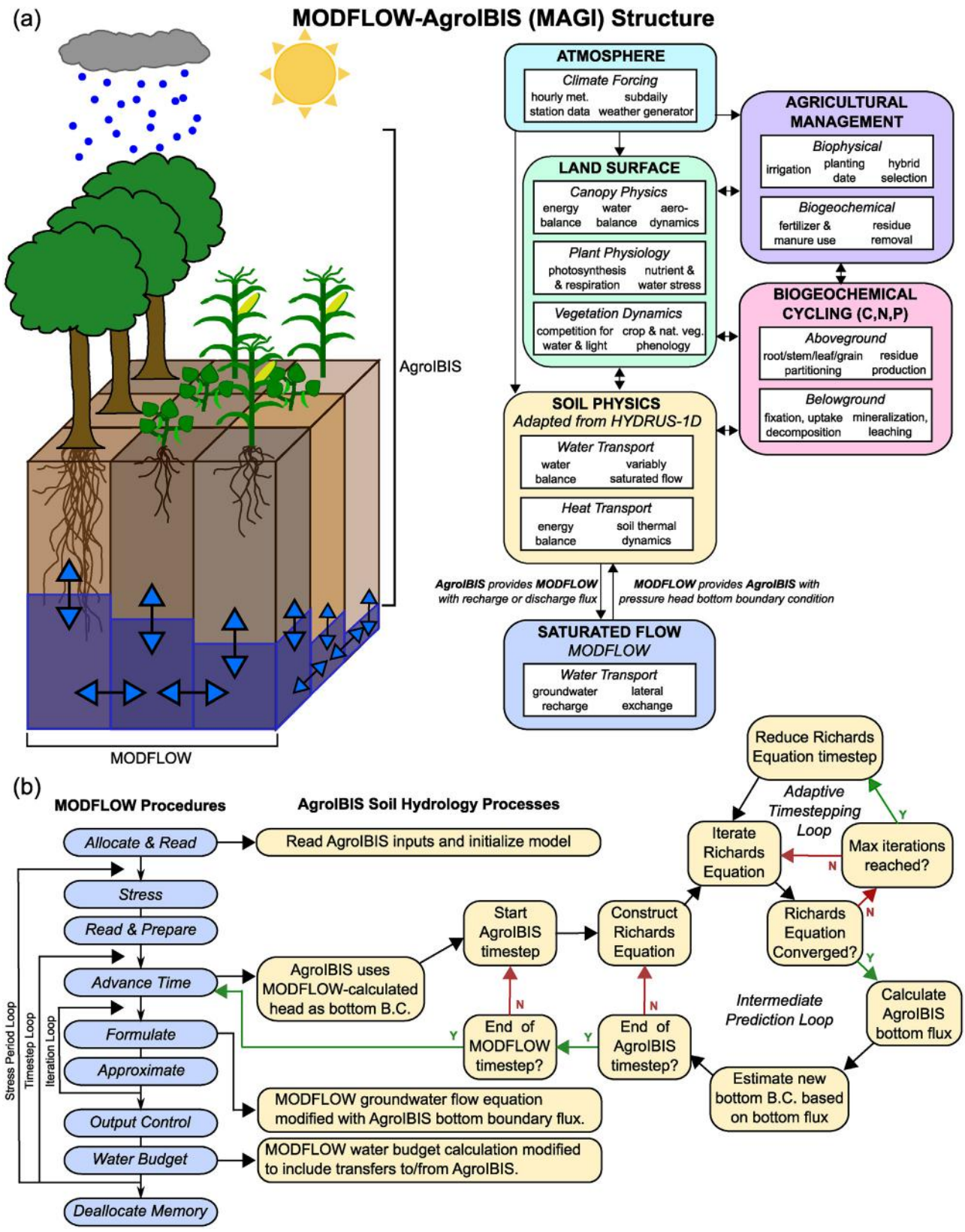

Fig. 1. (a) Conceptual overview of MAGI including key processes. (b) Flowchart showing coupling structure between MODFLOW and AgroIBIS. Each box on the left represents a MODFLOW procedure (simplified from Harbaugh et al., 2005), and boxes on the right show where AgroIBIS interfaces with MODFLOW. "B.C." is short for "Boundary Condition".

Brye, 2003; Twine et al., 2004). Subsequent studies validated carbon and energy fluxes (Kucharik et al., 2006; Kucharik and Twine, 2007; Motew and Kucharik, 2013), snowpack accumulation and timing (Kucharik et al., 2013; Lenters et al., 2000; Twine et al., 2005; Vano et al., 2006), response to atmospheric CO_2 concentration (Twine et al., 2013), and plant phenology (Kucharik and Twine,

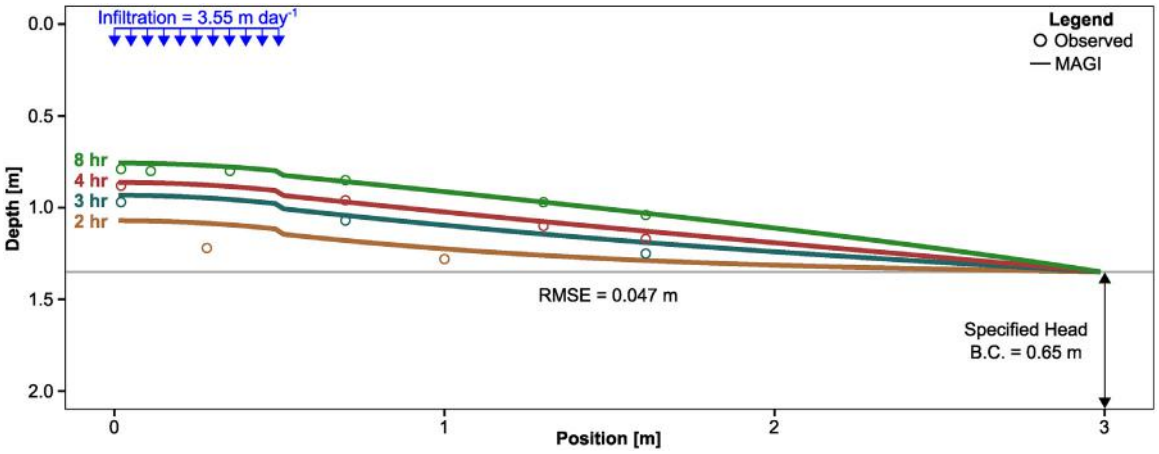

Fig. 2. Modeled (lines) and observed (circles) hydraulic head distributions for sandbox validation experiment at different times. Grey horizontal line shows initial water table. Observed data are from Vauclin et al. (1979).

2007; Twine et al., 2013; Webler et al., 2012; Xu et al., 2014). Additional PFTs including sugarcane (Cuadra et al., 2012), miscanthus (VanLoocke et al., 2010), and switchgrass (VanLoocke et al., 2012) have since been introduced to AgroIBIS.

Soylu et al. (2014) replaced the soil physics of the original AgroIBIS with the variably saturated soil water flow and heat transfer model HYDRUS-1D (Fig. 1a) (Šimůnek et al., 2013). This represents a substantial improvement over existing agroecosystem and dynamic vegetation models, as well as previous versions of AgroIBIS, which typically use a small number of thicker soil layers and a volumetric water content-based solution to the Richards Equation. The new AgroIBIS simulates soil hydrology and energetics using the one-dimensional mixed hydraulic head and volumetric water content-based Richards Equation for water movement (Richards, 1931):

$$\frac{\partial}{\partial z}\left[K\left(\psi\right)\left(\frac{\partial \psi}{\partial z}+1\right)\right]-S\left(\psi\right)=\frac{\partial \theta}{\partial t} \quad (1)$$

where K is the hydraulic conductivity in the z dimension [L T^{-1}], ψ is the pressure head [L], S is a sink term representing root water uptake [L^{-1}], θ is the volumetric water content [L^3 L^{-3}], and t is time [T]. θ and ψ are related by a soil water characteristic curve (Clapp and Hornberger, 1978; Van Genuchten, 1980). By solving the Richards Equation as a function of pressure head rather than volumetric water content, the mixed form of the Richards Equation allows AgroIBIS to accurately simulate the impacts of groundwater on the unsaturated zone, such as capillary rise. For a complete description and validation of the coupling between AgroIBIS and HYDRUS-1D, the reader is referred to Soylu et al. (2014) and Zipper et al. (2015). This approach was also validated at a watershed scale via comparison with streamflow, sediment yield, and soil/lake phosphorus concentrations when coupled with the THMB surface water routing model (Motew et al., 2017).

Vegetation within AgroIBIS is represented as two canopy layers populated by different plant functional types (PFTs) including natural forest, shrub, and grassland PFTs as well as agroecosystem PFTs. For each PFT, biophysically-based computations of photosynthesis, stomatal conductance, and respiration are used to simulate leaf physiology to calculate water and carbon exchanges at an hourly timestep (Collatz et al., 1991; Farquhar et al., 1980). Progression through plant phenological growth stages and carbon allocation is based on the accumulation of thermal time (i.e. degree days) and temperature thresholds, which dynamically vary during the growing season controlled by PFT-specific parameters. These time-varying parameters control carbon (C) allocation among leaf, stem, root, and grain pools. AgroIBIS calculates ET following Pollard and Thompson (1995) as the sum of total transpiration (from upper and lower canopies), evaporation of water intercepted by vegetation, and soil surface evaporation. Physiological parameterizations are used to defined PFT-specific sensitivity to stresses such as water, oxygen, and nitrogen deficiencies (Feddes et al., 1974, 1976), with rooting profiles for each PFT following an exponential distribution defined by the global parameters of Jackson et al. (1996). A detailed description of IBIS and AgroIBIS is available in a suite of studies introducing and validating the model (Foley et al., 1996; Kucharik, 2003; Kucharik et al., 2000; Kucharik and Brye, 2003; Kucharik and Twine, 2007; Soylu et al., 2014).

The latest version of AgroIBIS, introduced in Motew et al. (2017), also includes four urban PFTs (open space and low/medium/high density) aligned with the classes of the National Land Cover Dataset (Homer et al., 2015). These urban PFTs are represented using a hybrid of the AgroIBIS process-based algorithms and an empirical curve number approach (impervious areas only), similar to Arden et al. (2014) and Schneider et al. (2012). For urban PFTs, AgroIBIS simulates pervious areas as grass with a maximum permitted canopy height of 0.11 m. For this study, C4 grasses were used in urban areas, but other vegetation types (e.g. C3 grasses) can also be used depending on local vegetation communities. Separately, runoff from impervious areas is calculated in each urban cell using the NRCS Curve Number (CN) approach with CN set to 98 (United States Department of Agriculture, 1986). Estimates of runoff from AgroIBIS for pervious areas (based on the Richards Equation) and impervious areas (using the CN) are then weighted based on the relative fraction of impervious and pervious cover within each grid cell; defaults for MAGI are 0%, 10%, 35%, and 65% impervious cover for open, low, medium, and high-density urban areas, respectively. Rainfall on urban areas that is not runoff under the CN approach is added to ET as calculated by AgroIBIS to account for evaporation from impervious surfaces. Other model outputs and exchange fluxes with MODFLOW, such as groundwater recharge, capillary rise, nitrate leaching, ET, LAI, and biomass, are also scaled based on the proportion of impervious cover for each urban PFT.

AgroIBIS provides several advantages for the representation of land surface processes over other Richards Equation-based models. First, AgroIBIS is a dynamic vegetation model including the complete water, energy, and carbon cycles, designed for the explicit representation of natural and agroecosystems including major commodity and bioenergy crops. AgroIBIS estimates photosynthesis at hourly timesteps and uses accumulated carbon to simulate vegetation growth via partitioning into root, stem, leaf, and grain pools; critically, this allows for the simulation of crop yield, the

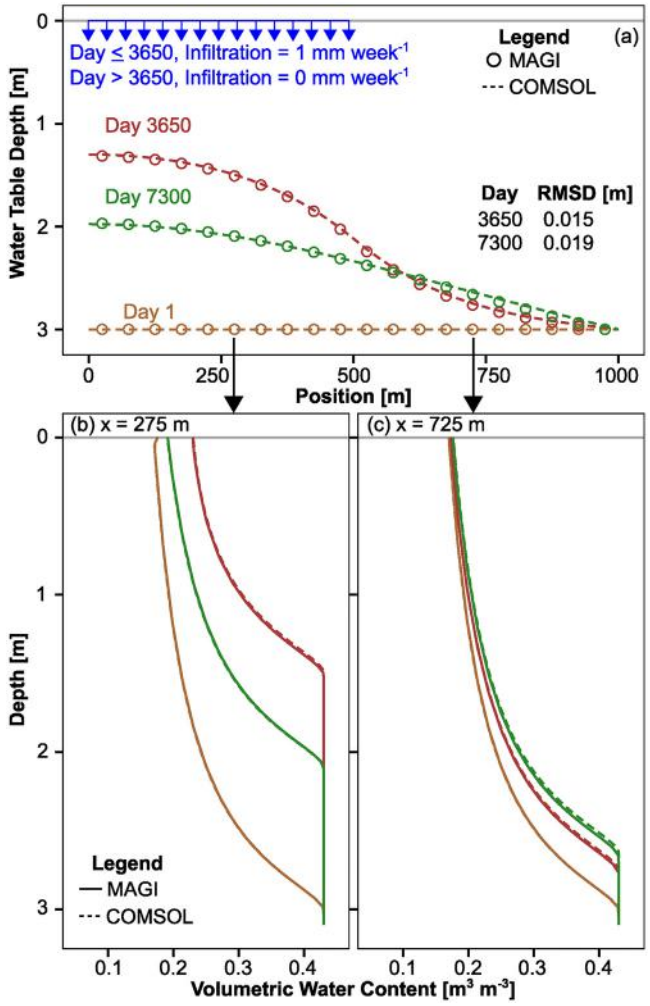

Fig. 3. Recharge mound validation of (a) cross-section of water table depth, and vertical profiles of soil moisture (b) under the wetting front and (c) outside of the wetting front.

key variable of interest to most farmers and global food production projections. Second, AgroIBIS simulates the complete nitrogen and phosphorus nutrient cycles in agroecosystems, including deposition, mineralization, plant uptake, leaching, and erosion. Combined, these advantages enable AgroIBIS to simulate the impacts of agricultural land use on critical zone processes in considerable detail at point to global scales, including the effects of management practices such as irrigation (Kucharik and Twine, 2007; Schneider et al., 2012; Twine and Kucharik, 2009), fertilizer and manure application (Donner et al., 2004; Donner and Kucharik, 2008, 2003; Kucharik and Brye, 2003), shifts in hybrid selection or planting date (Sacks and Kucharik, 2011), and residue management practices (Kucharik et al., 2013; Kucharik and Twine, 2007).

However, unlike other integrated surface-subsurface models, AgroIBIS does not dynamically couple surface and subsurface flow. Instead, runoff is calculated at individual grid cells, and AgroIBIS has previously been coupled with the Terrestrial Hydrology Model with Biogeochemistry (THMB) to include surface water and nutrient routing (Coe, 2000, 1998; Coe et al., 2008; Donner et al., 2004; Donner and Kucharik, 2003). This approach arose from AgroIBIS' original development as a global dynamic vegetation model with coarse (1°) grid cells, a spatial resolution at which runon is a subgrid level process. This lack of overland flow routing within AgroIBIS may make the model inappropriate for hillslope hydrology or fine spatial resolution studies where runoff/runon dynamics significantly impact the water balance within a vertical AgroIBIS grid cell. The present study does not include the coupled THMB model.

2.2. Coupling with MODFLOW

To provide a new tool for addressing interactions and feedbacks between groundwater and ecosystem processes with the explicit representation of dynamic vegetation growth, we coupled the AgroIBIS ecosystem model to the modular groundwater flow model, MODFLOW-2005 (Harbaugh, 2005); hereafter, we refer to the coupled models as MODFLOW-AgroIBIS (MAGI). MODFLOW-2005 (Harbaugh, 2005), is a version of the MODFLOW family of finite-difference groundwater flow models, which have been widely used and validated since being introduced in the 1980s (McDonald and Harbaugh, 1988). MODFLOW has been successfully applied at scales ranging from riparian floodplains (Doble et al., 2006; Faulkner et al., 2012; Mastrocicco et al., 2014; Zell et al., 2015) to watersheds (Cho et al., 2009; Falke et al., 2011; Lam et al., 2011; Sutanudjaja et al., 2011, 2014) to global (de Graaf et al., 2015, 2017).

MODFLOW simulates three-dimensional saturated groundwater flow for a porous medium using a block-centered finite-difference approach and solving the partial-differential equation:

$$\frac{\partial}{\partial x}\left(K_{xx}\frac{\partial h}{\partial x}\right)+\frac{\partial}{\partial y}\left(K_{yy}\frac{\partial h}{\partial y}\right)+\frac{\partial}{\partial z}\left(K_{zz}\frac{\partial h}{\partial z}\right)-W=S\frac{\partial h}{\partial t} \quad (2)$$

where K_{xx}, K_{yy} and K_{zz} are values of hydraulic conductivity in the x, y, and z directions [L T^{-1}]; h is the potentiometric head [L]; W is a volumetric flux per unit volume representing sources and/or sinks of water, e.g. pumping wells [T^{-1}]; S is the storage coefficient accounting for elasticity of the porous material [L^{-1}]; and t is time [T] (Harbaugh, 2005). MODFLOW is designed and built around the concept of modular programming, in which specific packages simulate different components of groundwater flow systems. Existing packages simulate processes including solute transport (Guo and Langevin, 2002; Hornberger et al., 2002; Zheng et al., 2001), groundwater management (Ahlfeld et al., 2005), aquifer subsidence (Hoffmann et al., 2003), and interactions with surface water features (Merritt and Konikow, 2000; Niswonger and Prudic, 2005; Prudic et al., 2004).

To couple AgroIBIS and MODFLOW, we converted AgroIBIS to a MODFLOW package. Similar to the HYDRUS package for MODFLOW (Seo et al., 2007), AgroIBIS simulates all land surface and unsaturated zone processes, and calculates the average flux across the bottom of the soil profile for each MODFLOW timestep. This flux is passed to MODFLOW as a source/sink (W in Eq. (2)) to the upper layer of the groundwater flow equation. MODFLOW then solves the groundwater flow equation to calculate a new hydraulic head distribution over the model domain, which is provided to AgroIBIS as a pressure head bottom boundary condition corresponding to the height of the water table above the bottom of the AgroIBIS soil profile. Within this coupled framework, all changes in storage due to the draining and filling of pore spaces occur within the AgroIBIS soil column via the response of the pressure head profile to changes in the bottom boundary condition and corresponding changes in soil moisture; within MODFLOW, only storage changes resulting from aquifer and fluid compression/expansion are represented. Thus, all AgroIBIS cells must be discretized such that hydraulic head never drops below the bottom of the soil profile during a simulation.

MAGI simulates myriad processes within a single modeling framework and these processes operate at timesteps ranging from minutes to years. "Fast" processes (e.g. near-surface fluxes of energy, water and momentum, photosynthesis, and respiration) operate at timesteps of minutes to hours; "medium" processes (e.g. vegetation phenology and carbon/nutrient cycling) operate

at timesteps of days to weeks; and "slow" processes (e.g. agricultural management, planting decisions, and land cover transitions) operate at monthly to yearly timesteps. In MAGI, these processes are organized in a hierarchical framework allowing each process to operate internally at the proper timestep, while the coupling between AgroIBIS and MODFLOW is designed in a way such that the groundwater flow equation can be solved at a user-defined frequency as determined by the needs of a particular simulation. For example, in simulations where lateral flow is expected to change slowly and/or groundwater is expected to be relatively unimportant to ecosystem processes, the groundwater flow equation can be solved at weekly or longer timesteps, while in applications where hydraulic conductivity is very high or lateral groundwater flow is very important, MODFLOW and AgroIBIS can exchange fluxes hourly.

One issue associated with differences in timestep length between AgroIBIS and MODFLOW is that holding a constant pressure head bottom boundary condition in AgroIBIS for an entire MODFLOW timestep can lead to overestimates of groundwater recharge or capillary rise, causing oscillatory groundwater table dynamics over time. To eliminate these issues, we implemented an intermediate prediction mechanism into the coupling between AgroIBIS and MODFLOW, shown in Fig. 1b. This prediction mechanism estimates a new AgroIBIS bottom boundary condition based on the storage coefficient of the uppermost MODFLOW layer and the calculated bottom boundary flux each time the Richards Equation is solved, and which is used for the next Richards Equation timestep, and this process is completed until a new MODFLOW timestep is reached. At this point, the cumulative bottom boundary flux from AgroIBIS over the entire MODFLOW timestep is input into the MODFLOW groundwater flow equation, and the AgroIBIS bottom boundary condition is updated based on the new MODFLOW solution. Effectively, this prediction step can be thought of as approximating the groundwater response as one-dimensional in the vertical direction during each AgroIBIS timestep, with lateral flow occurring only during each MODFLOW timestep.

3. Model validation

To ensure accurate performance of MAGI, we conduct four validation tests. To test the Richards Equation solver, we simulate a 1D comparison to a field infiltration experiment described in Wierenga et al. (1991) (Fig, A1). To evaluate water table response to recharge and exchange between MODFLOW and AgroIBIS, we simulate a short-term 2D sandbox experiment (Vauclin et al., 1979) and a long-term 3D groundwater mounding scenario (Section 3.2). To evaluate groundwater impacts on land surface processes including exfiltration, we simulated a 3D tilted v-catchment benchmarking problem used as part of the Integrated Hydrological Model Intercomparison Project (IH-MIP; Kollet et al., 2017).

3.1. Sandbox experiment

We simulated a two-dimensional sandbox experiment described in Vauclin et al. (1979) in order to test MAGI's ability to simulate a changing water table in response to infiltration within a subset of the domain. The model domain for this experiment is a sandbox with a depth of 2.0 m and a width of 6.0 m; as the experiment was symmetrical, we only simulated half of the domain, for a width of 3.0 m (Fig. 2; Twarakavi et al., 2008). The entire domain had an initial head of 0.65 m and the initial pressure head and soil moisture distributions were assumed to be in hydrostatic equilibrium. For a period of 8 h, infiltration was applied to the leftmost 0.5 m of the domain at a rate of 4.11×10^{-5} m s^{-1} (3.55 m d^{-1}). We discretized the model into 150

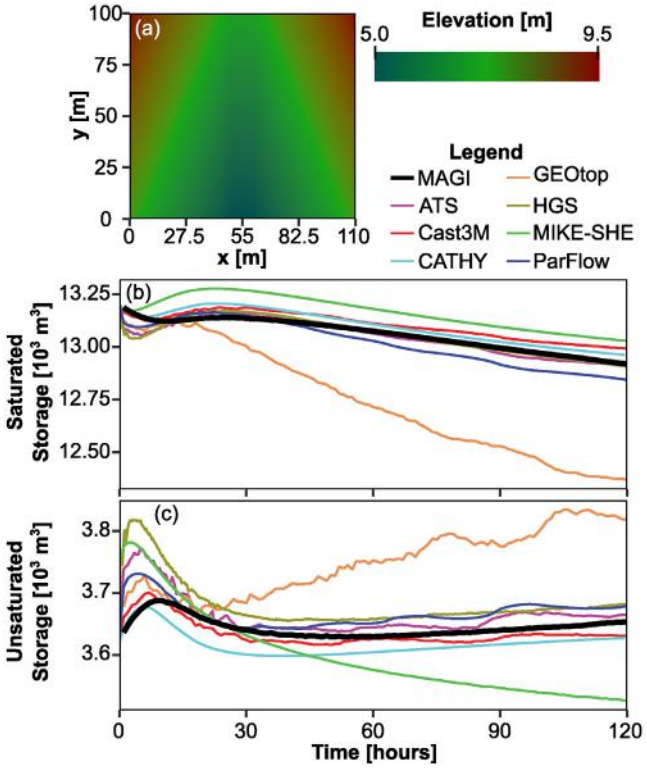

Fig. 4. Tilted v-catchment validation. (a) Elevation of land surface for model domain. Total volume in (b) saturated and (c) unsaturated storage through time. Data for all models besides MAGI are from Kollet et al. (2017).

cells of 0.02 m width, with a no-flow boundary on the left (x=0 m) and a specified head boundary of 0.65 m on the right (x=3.0 m). Soil hydraulic properties were the same in the unsaturated and saturated zones and were provided by Vauclin et al. (1979) as follows: saturated hydraulic conductivity (K_{sat}) = 8.40 m d^{-1}, saturated volumetric water content (θ_s) = 0.300 m^3 m^{-3}, residual volumetric water content (θ_r) = 0.010 m^3 m^{-3}, Van Genuchten parameter α = 3.30 m^{-1}, and Van Genuchten parameter n = 4.10. As MAGI is not designed to run at sub-daily timesteps, we scaled one minute of experiment time to one day of model time, and adjusted all rates and conductivities accordingly.

MAGI predicts a more rapid than observed rise in the water table early in the experiment, but closely matches the observed data at the end of the experiment, for an overall RMSE of 0.047 m (Fig. 2). We attribute the discrepancy between MAGI and observations early in the experiment to a lack of lateral flow in the unsaturated zone in MAGI. Due to the extremely high infiltration rate, experimental results showed a significant horizontal component to the wetting front relative to the limited horizontal extent of the domain, while the one-dimensional nature of AgroIBIS forced the wetting front to move only vertically. This led to greater recharge in MAGI compared to the observations early in the experiment. As vertical flow becomes the dominant vadose zone process later in the experiment, the agreement between the model and experiment results improves.

3.2. Recharge mound experiment

To test MAGI's coupling between the unsaturated and saturated zones in a setting more representative of the 3D, landscape-scale simulations MAGI is designed for, we designed a hypothetical experiment where a pulse of infiltration was applied to the land surface for 10 years, followed by 10 years with no infiltration. We compared MAGI and COMSOL simulations to assess the impact

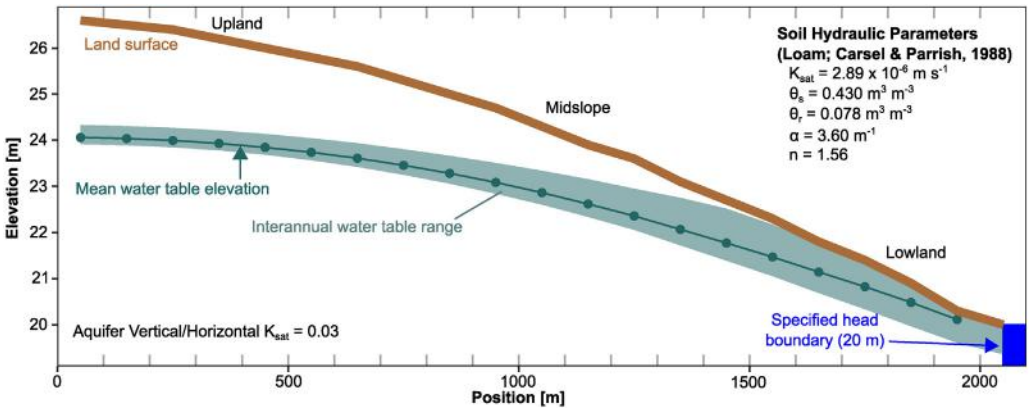

Fig. 5. Conceptual model of domain used for urbanization scenarios. Ticks along bottom and top show domain discretization. Uplands, midslope, and lowland regions correspond to terms used in text to refer to leftmost, central, and rightmost portions of domain, respectively.

of neglecting lateral flow in the unsaturated zone using MAGI in larger domains relevant to terrestrial ecosystem processes. The experimental design is a 1000 m × 1000 m domain, discretized into 100 cells with a width and height equal to 100 m (Fig. 3). The left (x = 0 m) and top (y = 0 m) edges of the domain were no-flow boundaries, the right (x = 1000 m) and bottom (y = 1000 m) edges were specified head boundaries at an elevation of 17.0 m, and the domain had a uniform height of 20.0 m with hydrostatic initial conditions. In one quadrant of the domain (x < 500 m; y < 500 m), infiltration was defined at a rate of 1.65×10^{-9} m s^{-1} (1 mm $week^{-1}$) for the first 10 years of the simulation, and 0 for the next 10 years of the simulation. All other surface fluxes were set to zero. Soils in both the saturated and unsaturated zones were parameterized as a homogeneous loam using the mean values provided by Carsel and Parrish (1988).

Results from the recharge mound validation experiment demonstrate that the hydraulic head and soil moisture response is comparable between MAGI and COMSOL both underneath and away from the infiltration zone (Fig. 3), despite MAGI's lack of lateral flow in the unsaturated zone. The root mean squared difference (RMSD) of hydraulic head between MAGI and COMSOL is <0.02 m during both the rising and falling phases of the water table, and the lateral hydraulic gradient is well-captured, including a rising water table in areas outside of the infiltration zone. As these areas did not receive any direct infiltration, the rise in the water table (and accompanying increase in soil moisture in the unsaturated zone) can be attributed to lateral flow through the saturated zone and capillary rise from the saturated zone into the unsaturated zone.

3.3. Tilted v-catchment experiment

Finally, we compared MAGI to a 3D tilted v-catchment benchmark used by the second phase of the Integrated Hydrologic Model Intercomparison Project (IH-MIP2; Kollet et al., 2017). This benchmark problem is intended to validate interactions between surface and subsurface water during 120 h of recession from an initially non-equilibrium water table. The domain is 110 m in the x-dimension and 100 m in the y-dimension, and consists of two slopes surrounding a 10 m thick central channel (Fig. 4a). Our MAGI model had a uniform vertical thickness of 5 m and an initial hydrostatic pressure head profile for each grid cell with a water table depth of 2 m. We discretized the model into 11,000 grid cells in the lateral dimension with a resolution of 1 m in both the x- and y-dimensions, and 150 soil layers in the vertical dimension with linearly increasing thickness from a minimum of 0.005 m at the land surface to a maximum of 0.061 m at the bottom of the soil column. Soil hydraulic properties were defined based on Kollet et al. (2017) as follows: K_{sat} = 240 m d^{-1}, θ_s = 0.400 m^3 m^{-3}, θ_r = 0.080 m^3 m^{-3}, α = 6.0 m^{-1}, and n = 2.0. As in the sandbox experiment (Section 3.1), we scaled conductivities and rates to work within AgroIBIS' daily timestep such that one hour of experiment time was equal to one day of model time.

MAGI was validated via comparison to the integrated surface-subsurface models that participated in IH-MIP2: Advanced Terrestrial Simulator (ATS; Painter et al., 2016), Cast3 M (Weill et al., 2009), CATchment HYdrology (CATHY; Bixio et al., 2002; Camporese et al., 2010), GEOtop (Endrizzi et al., 2014; Rigon et al., 2006), HydroGeoSphere (HGS; Aquanty Inc., 2015), MIKE-SHE (Abbott et al., 1986; Butts et al., 2004), and ParFlow (Ashby and Falgout, 1996; Kollet and Maxwell, 2006; Maxwell and Miller, 2005). Note that we do not compare to outlet discharge or surface storage results from IH-MIP2, as MAGI does not include overland flow routing. More detailed descriptions of each of these models, as well as the tilted v-catchment domain, are available in Kollet et al. (2017) and references therein.

MAGI performs comparably to other integrated surface-subsurface models throughout the simulation period, despite MAGI's lack of runon capabilities, 1D unsaturated zone, and relatively coarse timestep (Fig. 4). At the start of the simulation, there is a slight decrease in saturated storage and increase in unsaturated storage as the water table begins to equilibrate laterally. After ~25 h, water begins to exfiltrate across the soil surface, forming puddles and generating runoff. As the water table recedes from ~25 h to the end of the simulation, saturated storage decreases and unsaturated storage increases slowly at a rate comparable to most of the rest of the models simulated.

In sum, these validation experiments demonstrate that the components constituting MAGI are appropriately coupled to capture feedbacks between the land surface, unsaturated zone, and groundwater domains. However, MAGI may not be well-suited to environments where groundwater is expected to be important at timescales smaller than the minimum coupling timestep between AgroIBIS and MODFLOW (one hour), e.g. areas with very high hydraulic conductivity; or domains where runon can be an important component of the water balance, e.g. hillslope hydrology applications with local topographic lows.

4. Model application

4.1. Urbanization experimental design

To demonstrate the capabilities of MAGI, we conducted a suite of simulations exploring feedbacks between LULC change (urbanization), groundwater recharge, subsurface flow, and agroecosystem

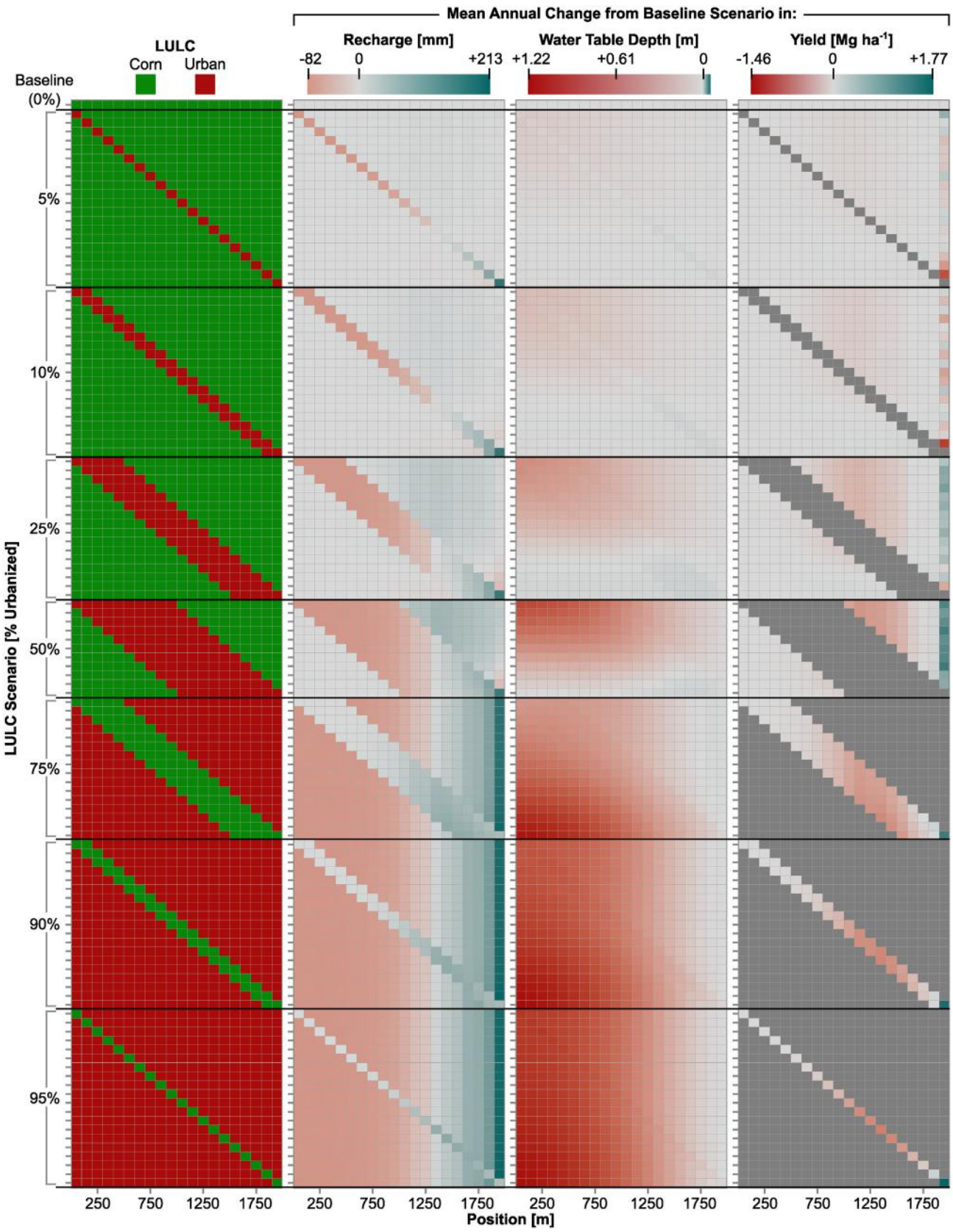

Fig. 6. Left column shows LULC scenarios; each of the 121 rows is a unique scenario simulated, and percentage labels correspond to the urban cover. Following columns show changes from baseline for each row: change in mean annual recharge (center-left; net recharge can be greater than 0, indicating capillary rise), change in mean WTD (center-right; positive value means deeper water table), and change in mean annual yield (right). Dark gray boxes in right column corresponds to urban cells where yield is not simulated.

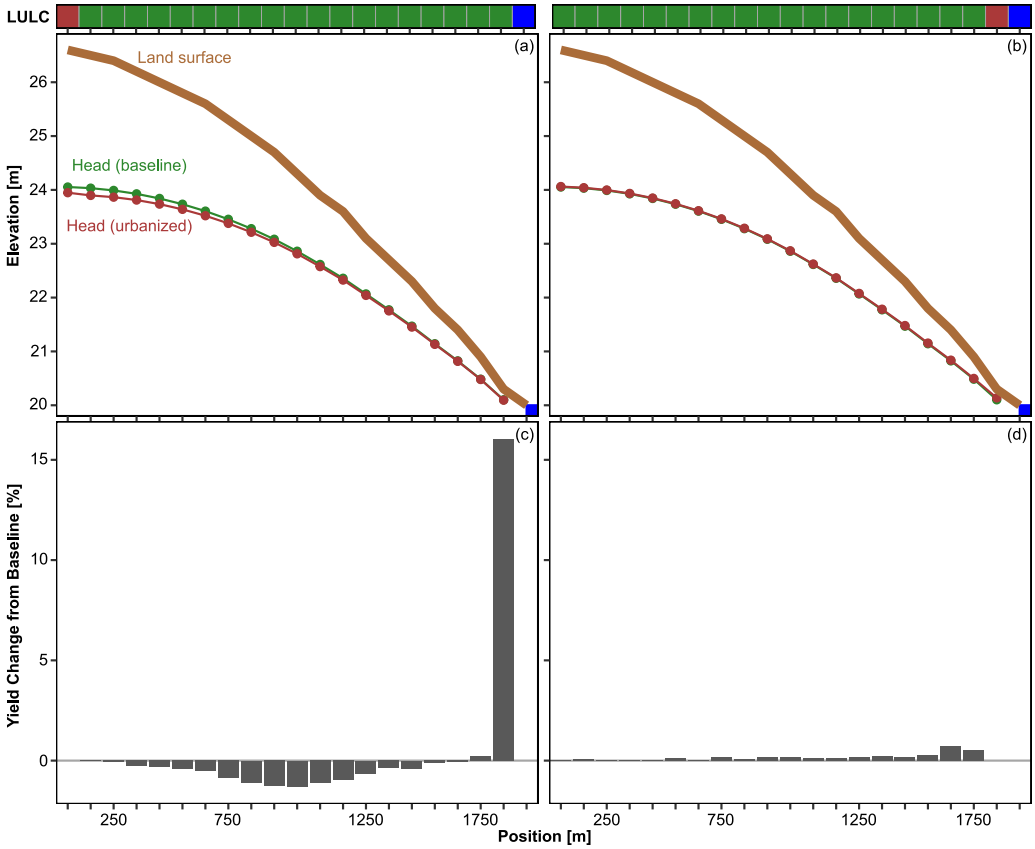

Fig. 7. (a,b) Mean head in both baseline scenario and urbanization scenario shown in bar along top; colors the same as Fig. 6. (c,d) Yield change at each location in urbanization scenario relative to baseline condition. Yield change at urbanized location and specified head boundary are not plotted because corn is not simulated there.

productivity (corn yield). Our domain was a two-dimensional (x-z) cross-section with unit thickness through an archetypal watershed bounded by a no-flow boundary condition on the left (x=0 m) and a specified head boundary of 20.0 m on the right (x=2100 m) (Fig. 5). The domain was discretized into 21 cells of 100 m width in the x dimension. The land surface elevation varied from 26.6 m on the left to 20.0 m on the right. To determine the initial head distribution, a starting groundwater elevation of 20.0 m was applied at all cells, and the model was run for 200 years using 2012 meteorological data (air temperature, wind speed, relative humidity, solar radiation, and precipitation) inputs from the University of Wisconsin Arlington Agricultural Research Station (43.31°N, −89.38°E) under homogeneous corn LULC. Initial head conditions were then specified for each cell, ranging from 25.4 m on the left to 20.0 m on the right, leading to an initial water table depth (WTD) range of 0–1.2 m. The 2012 growing season was selected for our simulations as it was characterized by severe drought in south-central Wisconsin, and therefore rainfed crops were exposed to water stress (Zipper et al., 2015; Zipper and Loheide, 2014). The topography and initial water table are such that they lead to oxygen stress at the shallow end of the spectrum and water stress where the WTD was deepest, thus capturing the full range of groundwater-yield interactions shown in Zipper et al. (2015).

Soil and aquifer hydraulic parameters were homogeneous within the AgroIBIS and MODFLOW domains, respectively. In the AgroIBIS portion of the model, we discretized the soil column into 200 soil layers ranging from a thickness of 0.005 m at the land surface to 0.146 m at a depth of 8.1 m. As in the recharge mound validation experiment, the vadose zone was parameterized as mean soil hydraulic properties for loam (Carsel and Parrish, 1988) with specific storage (S_s) of 10^{-5} m^{-1} and S of 0.005. For the MODFLOW portion of the domain, we defined a single unconfined aquifer layer with bottom elevation of 0.0 and a top elevation equal to the land surface. For this layer, we defined a horizontal hydraulic conductivity of 1.0×10^{-4} m s^{-1}, which is typical of glacially-derived sand and gravel aquifers in south-central Wisconsin, and a vertical/horizontal hydraulic conductivity anisotropy ratio of 0.03 so that vertical hydraulic conductivity in the saturated zone would be equal to vertical K_{sat} in the unsaturated zone. Modeled WTD is somewhat sensitive to the choice of coupling timestep between AgroIBIS and MODFLOW; care should be taken when selecting a coupling timesteps, as a timestep which is significantly longer than the timescales of relevant groundwater-ecosystem interactions may lead to a misrepresentation of both groundwater and ecosystem processes (Fig. A2). We use a daily coupling timestep between AgroIBIS and MODFLOW for all simulations described below.

Using this model architecture, we then simulated a suite of 121 urbanization scenarios which differ in both the percent of the landscape which is urbanized and the spatial configuration of urbanization (Fig. 6). Scenarios were developed by changing the PFT of a set percentage of the landscape (5–95%) from corn to medium-density urban, and moving the location of the urbanized cells (for urbanization <50% scenarios) or the corn cells (for urbanization >50% scenarios) across the landscape from uplands to lowlands. Each simulation was 50 calendar years in length but used repeated meteorological data from 2012. The first 30 years of each simulation for each scenario was a spin-up period with the corn PFT grown over the entire landscape to develop water and energy balances within the model at an approximate dynamic equilibrium. Following that, LULC in all urbanized cells was changed to the medium-density urban PFT for the final 20 years of the simulation. We also simulated

corn grown over the entire domain for the full 50 years (0% urbanization) as a baseline scenario for comparison with the urbanization scenarios. For all scenarios, output variables (recharge, water table depth, yield) were averaged over the final 10 years of each simulation. Fig. A3 shows the spin-up and change in WTD for a sample urbanization scenario and illustrates the model reaching dynamic equilibrium.

4.2. Impact of urbanization on vertical water balance

We find significantly spatial variability in the vertical water balance both under baseline conditions and urbanization scenarios. Under baseline conditions, simulated recharge (defined as the vertical flux between MODFLOW and each 1D AgroIBIS soil column) varied from –275 mm/year to +160 mm/year, indicating that a range of groundwater-ecosystem interactions are occurring including both groundwater recharge (recharge > 0) and discharge via capillary rise (recharge < 0). We attribute this variability in the vertical water balance under homogeneous land cover to differences in WTD at different landscape positions, leading to changes in the magnitude of groundwater contribution to evapotranspiration (Lowry and Loheide, 2010; Wang et al., 2016; Wu et al., 2015)

Across all simulations, we find that urbanization leads to changes in mean annual recharge ranging from –81 mm/year to +212 mm/year, with changes occurring both in locations where urbanization occurs as well as elsewhere in the domain (Fig. 6, 2nd column). In scenarios with <50% urbanization, changes in the vertical water balance are generally confined to the locations which were urbanized. When urbanization occurs in upland areas where the water table is deep relative to rooting depths, groundwater recharge decreases due to increased runoff resulting from the increase in impervious cover associated with urbanization. In contrast, when urbanization occurs in the lowland portion of the domain where the water table is shallow, the reduction in pervious area decreases ET and root water uptake, which leads to less capillary rise from the water table to the root zone and an apparent increase in groundwater recharge. This is consistent with previous studies which have found that shallow groundwater can significantly contribute to plant water requirements via both capillary rise and direct uptake (Han et al., 2015; Liu et al., 2016; Talebnejad and Sepaskhah, 2015; Wu et al., 2015), and demonstrates that plant water use can locally suppress the water table.

In scenarios with >50% urbanization, impacts of urbanization on the vertical water balance are apparent even in locations which remain corn, including decreases in groundwater recharge in upland areas and increases in groundwater recharge (same as decreases in groundwater discharge) in lowland areas when urbanized (Fig. 6, 2nd column). Slight increases in groundwater recharge also occurred in midslope areas where urbanization did not occur because the slight decrease in the WTD resulting from urbanization (Section 4.3) elsewhere leads to a decrease in capillary rise and overall net increase in groundwater recharge. This provides further evidence that LULC change in one location can impact the vertical water balance of areas which remain unchanged.

4.3. Impacts of urbanization on WTD

Urbanization-induced changes to the vertical water balance can lead to substantial changes in WTD. Across all simulations, urbanization leads to changes in the mean annual WTD at a location ranging from –0.12 m (shallower water table) to +1.57 m (deeper water table), with an increase in overall WTD in the majority of scenarios (Fig. 6, 3rd column). However, there is significant spatial variability in the sensitivity of WTD to urbanization across the landscape. WTD in the lowlands is relatively insensitive to changes in LULC elsewhere, while in the uplands WTD can get deeper by over

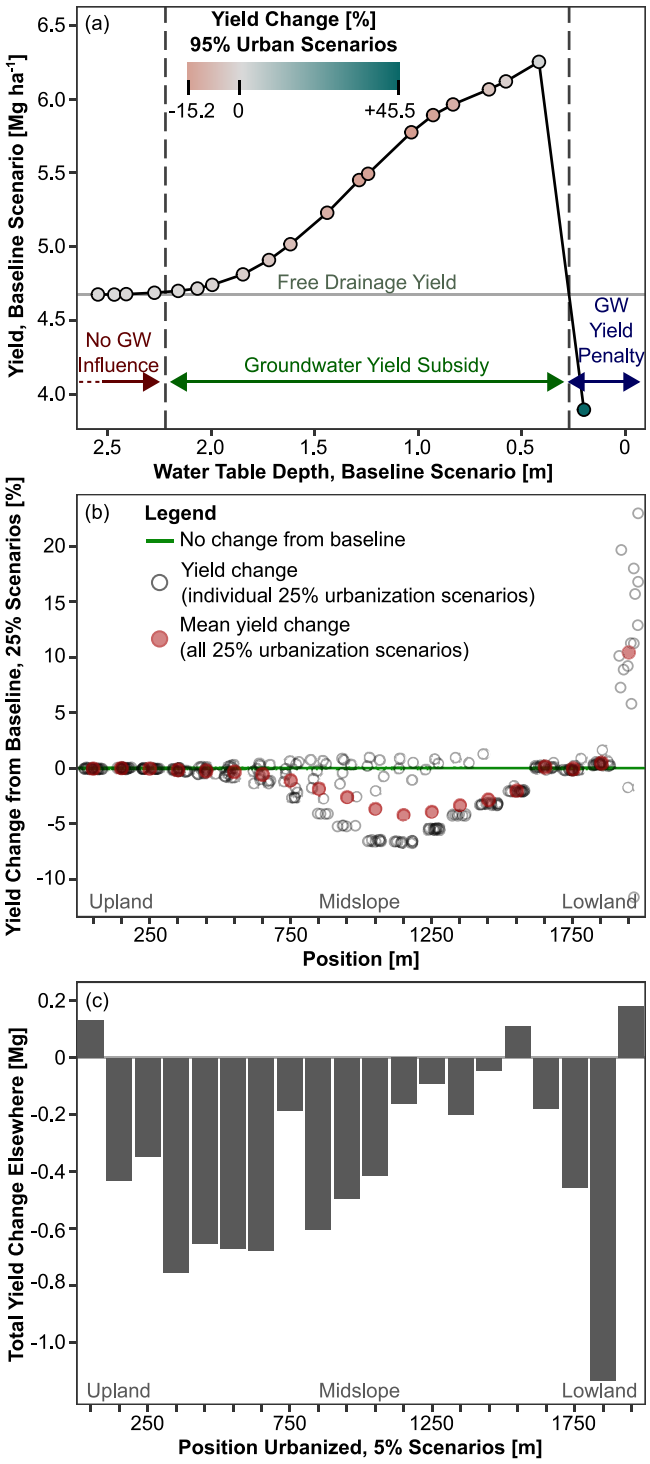

Fig. 8. Response of yield to urbanization scenarios. (a) Yield as a function of water table depth, with points color-coded by magnitude of yield change in the 95% scenario in which that point remains corn. Dashed lines correspond to groundwater-yield relationships (No Groundwater Influence, Groundwater Yield Subsidy, and Groundwater Yield Penalty) proposed by Zipper et al. (2015). (b) yield response at each location for all 25% urbanization scenarios; other urbanization scenarios are shown in Fig. A3. Black dots show all simulations in which a position remains corn, and red dots are the mean of all simulations for each position. (c) Cumulative yield change elsewhere on the landscape resulting from urbanization at each position, using cell depth of 100 m to convert cross-sectional yield changes to areal totals (each cell = 1 ha). (For interpretation of the references to colour in this figure legend, the reader is referred to the web version of this article.)

a meter. In particular, reductions in recharge in the uplands associated with urbanization exert a strong influence on WTD, both in the location where urbanization occurred and across the domain, as the water table responds to reductions in recharge to reach a new dynamic equilibrium (Fig. 7). These results complement the conclusions regarding groundwater irrigation drawn by Condon and Maxwell (2014), who found that water table drawdown due to groundwater abstraction in the lowlands was most strongly felt in upland areas where groundwater flow is diverging.

Using MAGI, we are able to investigate the ecohydrological interactions leading to the spatial variability in WTD response to urbanization. In lowlands, changes in WTD are small because of a negative feedback between three ecohydrological stabilizing mechanisms that occur in the lowlands. First, the specified head boundary on the right side of the domain (typical of a hydrologically connected stream or water body) provides a lateral source/sink of water and therefore prevents the water table from rising or falling substantially, regardless of changes in recharge elsewhere on the landscape. Second, plant root water uptake in the lowlands acts as a sink that extracts water from the unsaturated zone and inhibits the water table from rising far into the root zone during times when plant demand for water exceeds available precipitation. Third, water exits the soil domain via exfiltration when the water table rises to the land surface. Thus, the water table is relatively stable in the lowlands because excess water is removed via root water uptake and exfiltration, and water can be either provided or removed via lateral inflow from the specified head boundary (Fig. 7). In contrast, WTD in the uplands is highly sensitive to changes in the vertical water balance because the stabilizing feedbacks that keep the water table in a relatively narrow range in the lowlands are not active here.

These conclusions support previous research showing that changes in the vertical water balance associated with LULC change can alter the WTD at a landscape scale, which can lead to significant negative impacts including salt mobilization and landscape-scale flooding (Giménez et al., 2016; Kuppel et al., 2015; Nosetto et al., 2015). Our results extend these previous findings by demonstrating that LULC change can lead to contrasting water table responses depending on the prevailing ecohydrological dynamics at a location. In areas where the water table is constrained to a relatively narrow range by sources and sinks of water (in our example, streams and root water uptake) or groundwater convergence, changes in LULC can have a significant impact on the vertical water balance. However, the changes in the vertical water balance only have a localized impact on the water table because they do not lead to changes in the landscape-scale water table gradient. In contrast, in areas where the water table is unconstrained due to divergence of groundwater flow (in our example, the uplands region), relatively small changes in the vertical water balance can alter the overall water table gradient, allowing the impacts of LULC change to propagate through the domain, leading to widespread changes in the WTD.

4.4. Impacts of urbanization on yield

Urbanization can have both positive and negative impacts on yield elsewhere in the watershed due to the altered water table dynamics discussed in section 4.3. Across all scenarios, yield changes relative to the baseline conditions range from −1.46 Mg ha^{-1} to +1.77 Mg ha^{-1} (−37.51% to +45.45%). Reductions in yield are the largest in the central portion of the domain, while increases in yield occur primarily in the lowlands; it is important to note that this does not align with the regions experiencing the largest change in WTD, which are concentrated in the uplands (Fig. 6, 4th column).

The spatial mismatch between changes in WTD and changes in yield occurs because yield response to urbanization depends not only on the magnitude of change in WTD at a location, but also the initial water table conditions. Following Zipper et al. (2015), the relationship between yield and WTD is nonlinear and can be divided into three zones: (1) where groundwater is very shallow, roots experience oxygen stress and yield is reduced ('groundwater yield penalty'); (2) where groundwater is near the optimum depth, it provides a supplemental source of water, and yield is increased ('groundwater yield subsidy'); and (3) where groundwater is very deep, it has no influence on land surface processes ('no groundwater influence') (Fig. 8a).

Our results indicate that yield response to urbanization elsewhere is the largest within the groundwater yield penalty and subsidy zones where the slope of the relationship between yield and WTD is the steepest (Fig. 8). In upland regions, the water table is sufficiently deep that groundwater has no impact on the root zone water balance, and therefore changes in WTD associated with urbanization have no impact on yield. In midslope areas, there is a negative correlation between yield and WTD, such that changes in LULC that increase WTD lead to decreases in yield. In the lowlands, yield is suppressed due to oxygen stress, which leads to a steep positive correlation between WTD and yield; therefore, increases in WTD associated with urbanization can lead to dramatic increases in yield. These results indicate that ecosystems in which groundwater exerts a strong influence over land surface processes under prevailing conditions, corresponding to the groundwater-controlled zones highlighted by Maxwell and Kollet (2008), are most susceptible to LULC change elsewhere; using the dynamic vegetation capabilities of MAGI, we are able to further understand the degree to which these changes in the water and energy balance manifest in ecosystem services of interest, such as crop yield. These varying relationships between WTD and yield mean that landscape position also impacts the amount of yield variability across urbanization scenarios (Fig. 8b). These dynamics are shown in Fig. 8b, using the 25% urbanization scenarios as an example (other urbanization scenarios are shown in Fig. A4). In the uplands ('no groundwater influence' zone), the initial water table is sufficiently deep that there are minimal yield losses associated with even a large increase in WTD. In contrast, in midslope areas between the optimum WTD (where yield is highest under the baseline case) and the 'no groundwater influence' zone, changes in the WTD can lead to increases in yield if the water table gets shallower or decreases in yield if the water table gets deeper. This contributes to increased yield variability in response to urbanization elsewhere, in which different urbanization scenarios can have positive, neutral, or negative impacts on yield in the midslope region. This range of potential outcomes highlights the need to consider LULC as a landscape-level ecohydrological management opportunity. Averaging all scenarios, however, yield in midslope regions decreases under the conditions simulated. Similarly, in areas where yield is low due to oxygen stress ('groundwater yield penalty' zone), small changes in WTD can have a large impact because of the steep response of yield to very shallow groundwater by either raising the water table (yield decrease) or lowering the water table (yield increase).

There is also substantial spatial variability in the degree to which urbanization at a location influences yield elsewhere (Figs. 7 ; 8 c). Urbanization in the uplands leads to a net reduction in yield over most of the landscape, but a large increase in yield in the lowlands. In contrast, urbanization in the lowland areas induces net increases over most of the landscape, though of a smaller magnitude. These contrasting spatial signals exist because urbanization in the uplands causes a reduction in groundwater recharge (Fig. 6) which propagates laterally as a lower water table across the entire domain (Fig. 7). Lowering the water table leads to a small but consistent negative yield response through the entire midslope portion of the landscape due to a reduction in the groundwater yield subsidy, and an increase in yield in the lowlands where yield is suppressed

due to a groundwater yield penalty. In contrast, urbanization in the lowlands decreases total root water uptake, leading to a slightly shallower water table upgradient and relatively small yield gains due to reduced water stress (Fig. 7). The largest observed changes in yield occur when the cell immediately next to the cell experiencing a groundwater yield penalty; this is because urbanizing in this location reduces ET, leading to a decrease in WTD and increase in oxygen stress for neighboring locations. In general, however, effects of urbanization in lowland areas are relatively local due to the stabilizing ecohydrological feedbacks described in section 4.3. Therefore, urbanization in the lowlands leads to a large change in the vertical water balance at the cell being urbanized (Fig. 6), but relatively small effects on yield over most of the landscape because these changes do not propagate through and strongly impact the landscape-scale water table regime.

5. Discussion

Increasing the provision of desired ecosystem services while avoiding ecosystem disservices requires weighing landscape-scale tradeoffs between various LULCs (Booth et al., 2016; Graves et al., 2016; Qiu and Turner, 2013, 2015). Based on our results, we argue that maximizing positive outcomes (and/or minimizing negative impacts) of LULC change requires a process-based understanding of changes to the vertical water balance and/or ecosystem productivity caused by LULC-induced changes to the vertical water balance elsewhere on the landscape. Lateral groundwater-mediated impacts on land surface processes induced by LULC change elsewhere provide an opportunity for smart landscape-scale water management. For example, infiltration policies for new development focusing on the upland portions of watersheds may have the largest (positive or negative) impact on ecosystems elsewhere, while changes to LULC in areas where groundwater represents a large source of water for vegetation can have a large local impact but lesser lateral effects. From an ecological modelling perspective, new tools are needed that can quantify the degree to which LULC decisions in one location can impact ecosystem processes elsewhere on the landscape. By explicitly coupling groundwater flow processes to a state-of-the-art dynamic vegetation model, we demonstrate not just that lateral groundwater flow can be a key control over ecosystem processes, and also provide a new tool for studying these processes.

We acknowledge that groundwater recharge in urban environments is a complex and highly heterogeneous process, and our representation (which focuses solely on changes to the land surface and root zone) lacks processes that may be important locally. In this study, we have treated urbanization as a simplified process to gain insight into the impacts of change in the vertical water balance. In Baltimore, Bhaskar et al. (2015) found that the effects of infiltration/exfiltration from wastewater and water supply pipes on subsurface storage outweighed the impacts of either vegetation cover or impervious fraction. Similar impacts of pipe leakage have been observed or suggested in municipalities including Austin TX (Christian et al., 2011; Garcia-Fresca and Sharp, 2005) and Los Angeles CA (Townsend-Small et al., 2013). Furthermore, green infrastructural practices such as infiltration requirements for new developments, rain gardens, or disconnecting downspouts from impervious area can locally enhance infiltration and/or recharge (Newcomer et al., 2014; Shields and Tague, 2015), while private domestic wells can lead to local groundwater drawdown (Bhaskar et al., 2016). Where estimates of the relative importance of these factors are available, the framework of MAGI is sufficiently flexible to allow subsurface processes such as pipe leakage and domestic pumping to be implemented as source/sink terms to the flow equations, and processes such as urban irrigation to be represented as a surface flux.

Regardless, our fundamental point remains valid: changes in the vertical water balance induced by LULC change can impact land surface processes and ecological processes elsewhere via altered subsurface hydrology. While our results use an idealized test case to explore the potential direction and magnitude of these processes on yield during a dry year, impacts will likely vary based on factors including topography, hydrostratigraphy, agricultural practices, climate, and weather conditions (Soylu et al., 2014; Zipper et al., 2015, 2016a). We would therefore expect larger potential benefits from LULC-induced decreases in WTD in drier climates or during drought conditions, though these locations would also be most vulnerable to LULC-induced declines in groundwater levels. In contrast, yield losses due to a rising water table and enhanced groundwater yield penalties are likely to be greatest in wetter climates or rainier growing seasons.

Although further work is needed to identify and understand real-world scenarios in which these ecohydrological feedbacks exert a significant influence over processes of interest, our work demonstrates that modest changes to the vertical water balance induced by LULC change can impact land surface processes and ecological processes elsewhere via altered subsurface hydrology. Types of LULC change that have been shown to alter the vertical water balance and could therefore trigger these lateral feedbacks include deforestation (Amdan et al., 2013; Giménez et al., 2016), afforestation (Dean et al., 2015; Ilstedt et al., 2016; Nosetto et al., 2008), agricultural expansion or practices (Fan et al., 2016; Nosetto et al., 2015; Scanlon et al., 2005), biofuel expansion (Harding et al., 2016; VanLoocke et al., 2010, 2012), and urbanization (Bhaskar et al., 2015, 2016; Newcomer et al., 2014), among others. The strong impacts of urbanization on yield shown here highlight the need for ecological modellers to consider potential subsurface connections between areas when quantifying the response of ecosystems to environmental change.

6. Conclusions

We introduce MAGI, a new process-based critical zone modeling framework which couples the AgroIBIS land surface model, HYDRUS-1D variably saturated flow model, and MODFLOW groundwater flow model. While the case study covered here only simulates shallow groundwater flow, the modular nature of MODFLOW permits applications in layered and diverse groundwater flow systems. This powerful new modeling platform will allow for future exploration of feedbacks between ecological and subsurface processes, particularly as related to the impacts of LULC change and climate change on landscape-scale ecosystem services. We anticipate this will produce new insights regarding fundamental ecohydrological processes and be useful in addressing applied questions focusing on the impacts of management practices and land use decisions on both vertical and lateral components of the water budget, and the ecological implications thereof (e.g. from a restoration context).

Furthermore, we find that the impacts of urbanization on the vertical water balance, WTD, and agroecosystem yield are highly variable and governed by feedbacks between ecosystems and groundwater. Urbanization in upland areas, where groundwater has little influence on land surface processes, leads to decreases in groundwater recharge and reductions in WTD which propagate throughout the landscape via lateral groundwater flow, causing increased water stress in the midslope areas where yield had been more strongly enhanced by a groundwater yield subsidy. In contrast, while urbanization in lowland areas has a large impact on the vertical water balance, negative feedbacks between root water

uptake and lateral flow from nearby water sources prevent the impacts of LULC change in these regions from being felt broadly. Lateral impacts of changes in the vertical water balance represent an important but rarely considered impact of LULC change in three dimensions. Future work will move our understanding of these processes from the archetypal examples shown here to real-world conditions.

Acknowledgments

The authors were supported by the National Science Foundation Water Sustainability & Climate Program (DEB-1038759), the North Temperate Lakes Long-Term Ecological Research Program (DEB-0822700), and a University of Wisconsin-Madison Anna Grant Birge Award. We thank Mauro Sulis and Stefan Kollet for sharing IH-MIP2 data used for model validation. We gratefully acknowledge discussions with Eric Booth, Xi Chen, Dominick Ciruzzi, Melissa Motew, Mallika Nocco, Pavel Pinkas, Tracy Twine, Carolyn Voter, and Adam Ward during the model development process. Jeff McKenzie and the 2016 McGill University Groundwater and Water Resources seminar provided helpful feedback on an earlier version of this manuscript. We also appreciate comments from the editor and two anonymous reviewers, which significantly improved the quality of this manuscript.

Appendix A. Infiltration experiment validation

Infiltration experiment validation

We reproduced a field infiltration experiment described in Wierenga et al. (1991) to validate movement of water in the unsaturated zone. This experiment consisted of a trench face instrumented with neutron probes at various depths for soil water content measurement (Fig. A1). Water was applied to the ground surface via drip irrigation at a rate of 0.182 m day^{-1} for a total of 86 days, and the ground surface was covered to prevent evaporation or infiltration from precipitation. The water table was assumed to be deep enough to not affect soil hydrology within the trench.

We simulated this as a one-dimensional homogeneous soil column with a constant infiltration rate, following Twarakavi et al. (2008). Soil water retention characteristics were simulated using the Van Genuchten (1980) relationships and parameterized as follows: saturated hydraulic conductivity (K_{sat}) equal to 2.701 m d^{-1}; saturated volumetric content (θ_s) equal to 0.321 m^3 m^{-3}; residual water content (θ_r) equal to 0.083 m^3 m^{-3}; and fitting parameters (α and n) equal to 5.50 m^{-1} and 1.51, respectively. A uniform initial pressure head of −100 m was prescribed throughout the soil column and the water table was held constant at a depth of 12 m throughout the simulation; modeled pressure head profiles indicate that this deep water table had no effect on soil moisture in the zone of interest (<6 m).

We performed a complementary simulation with the same infiltration rate and soil hydraulic properties using the finite element solver COMSOL Multiphysics v5.2 (COMSOL, Inc., Burlington MA) for an intermodel comparison. COMSOL solves the three-dimensional Richards' Equation, meaning that lateral flow is included in the unsaturated zone, and is widely used in the hydro-

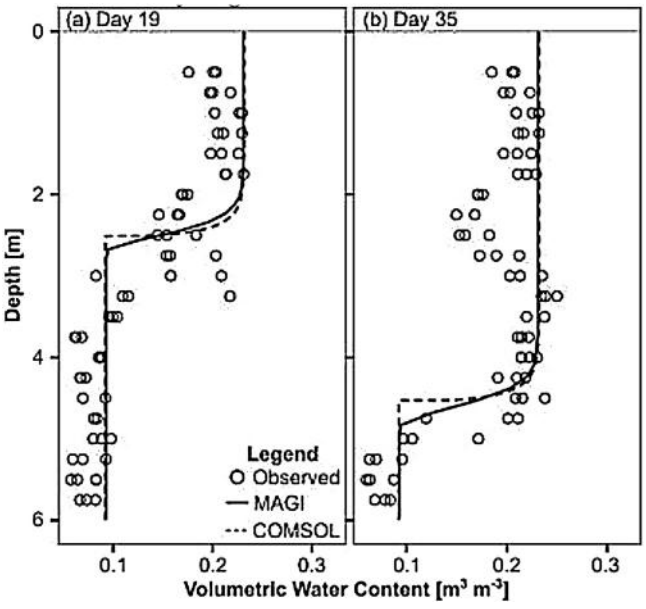

Fig. A1. Validation results from infiltration trench experiment on (a) day 19 and (b) day 35. Observed data are from Wierenga et al. (1991).

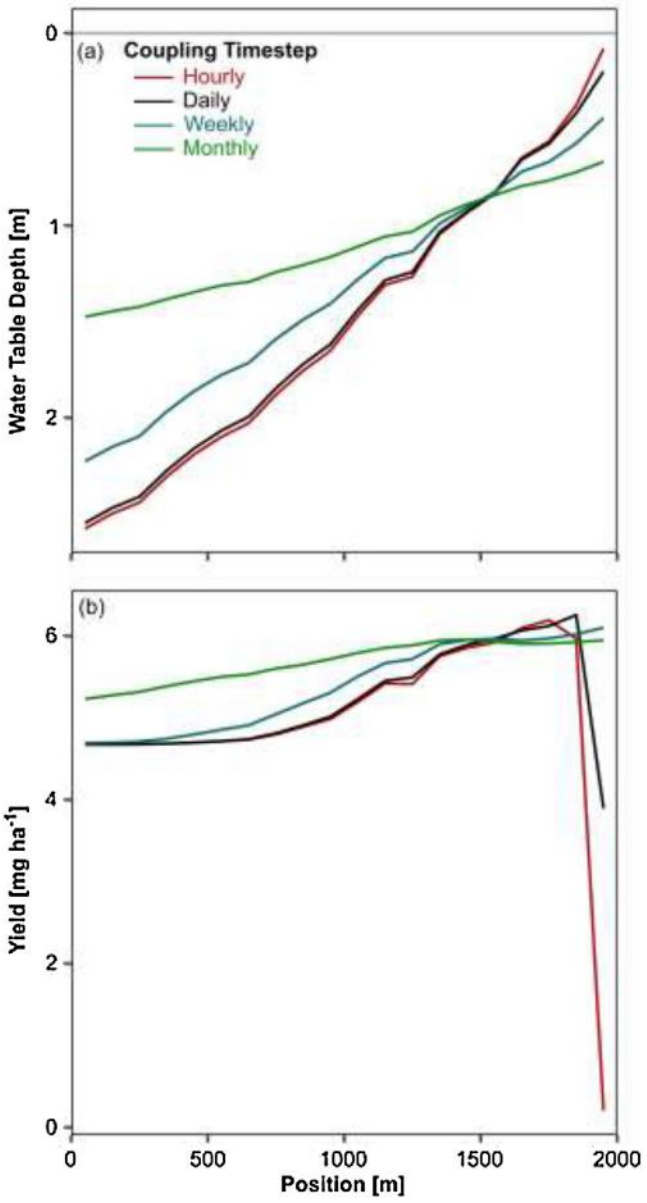

Fig. A2. Comparison of simulated (a) water table depth and (b) yield as a function of coupling timestep between AgroIBIS and MODFLOW. Lines show average over the final 10 years of the baseline simulation. All results in the manuscript use a daily coupling timestep.

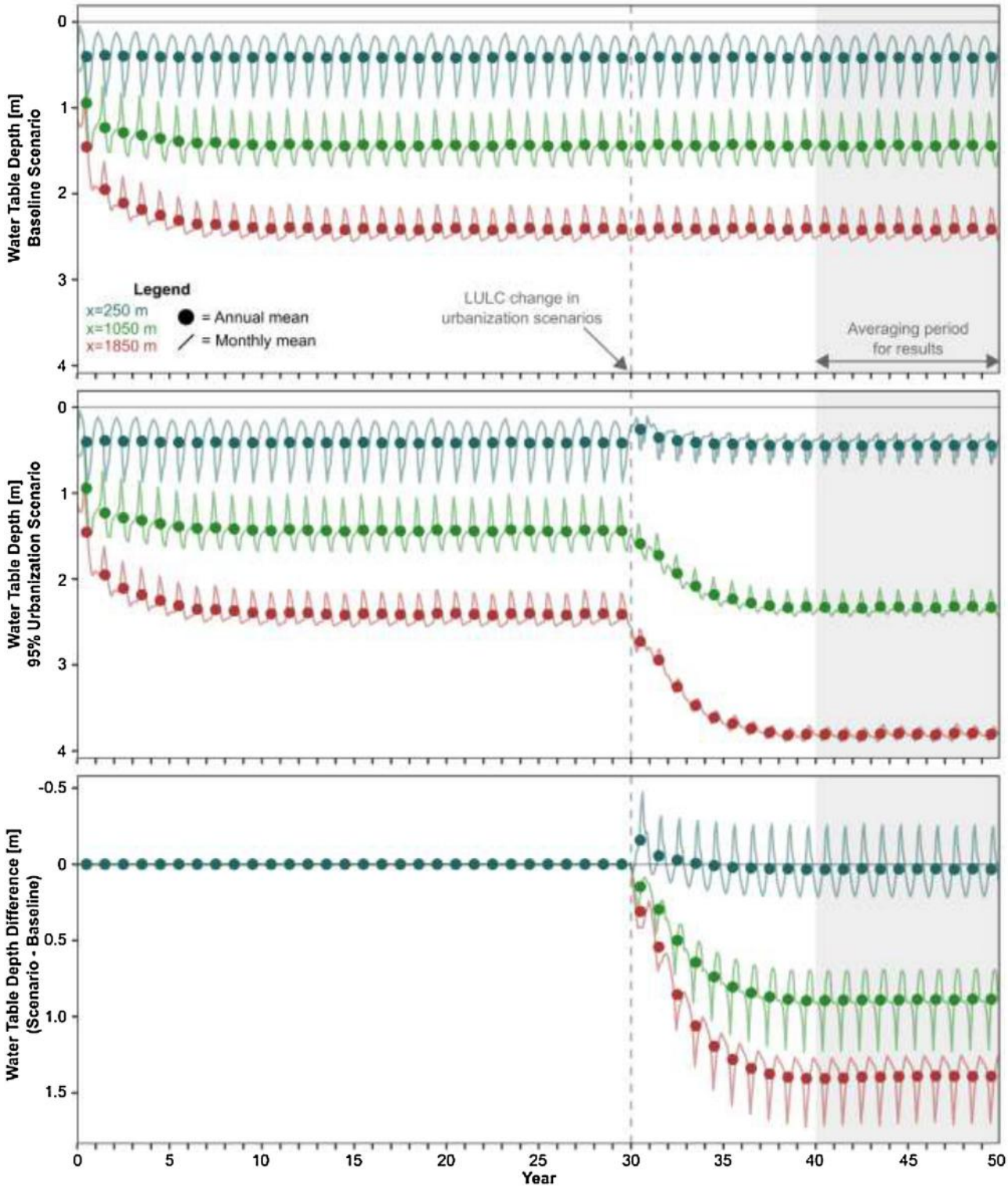

Fig. A3. Plots showing evolution of water table depth over time for 3 locations in the model domain for a sample 95% urbanization scenario (corn remains at position x = 1050 m). In each plot, lines show mean monthly WTD and points show mean annual WTD. The urbanization scenario begins at the dashed vertical line, and all results shown in figures are averaged over the shaded interval (last 10 years).

logical modeling community (Booth and Loheide, 2010, 2012; Cardenas, 2008; Gleeson et al., 2016; Sawyer et al., 2011; Singha and Loheide, 2011; Verma et al., 2014; Weber et al., 2013).

Results from the infiltration trench validation experiment shows that the wetting front is well captured in both space and time by both MAGI and COMSOL (Fig. A1), and our results are comparable to other unsaturated zone solvers (Twarakavi et al., 2008). The wetting front simulated by MAGI is more diffuse than that simulated by COMSOL and matches observed soil moisture data slightly better; this is because the discretization of soil layers is finer in COMSOL. Neither simulation captures variability in volumetric water content driven by subsurface variability in soil hydraulic properties

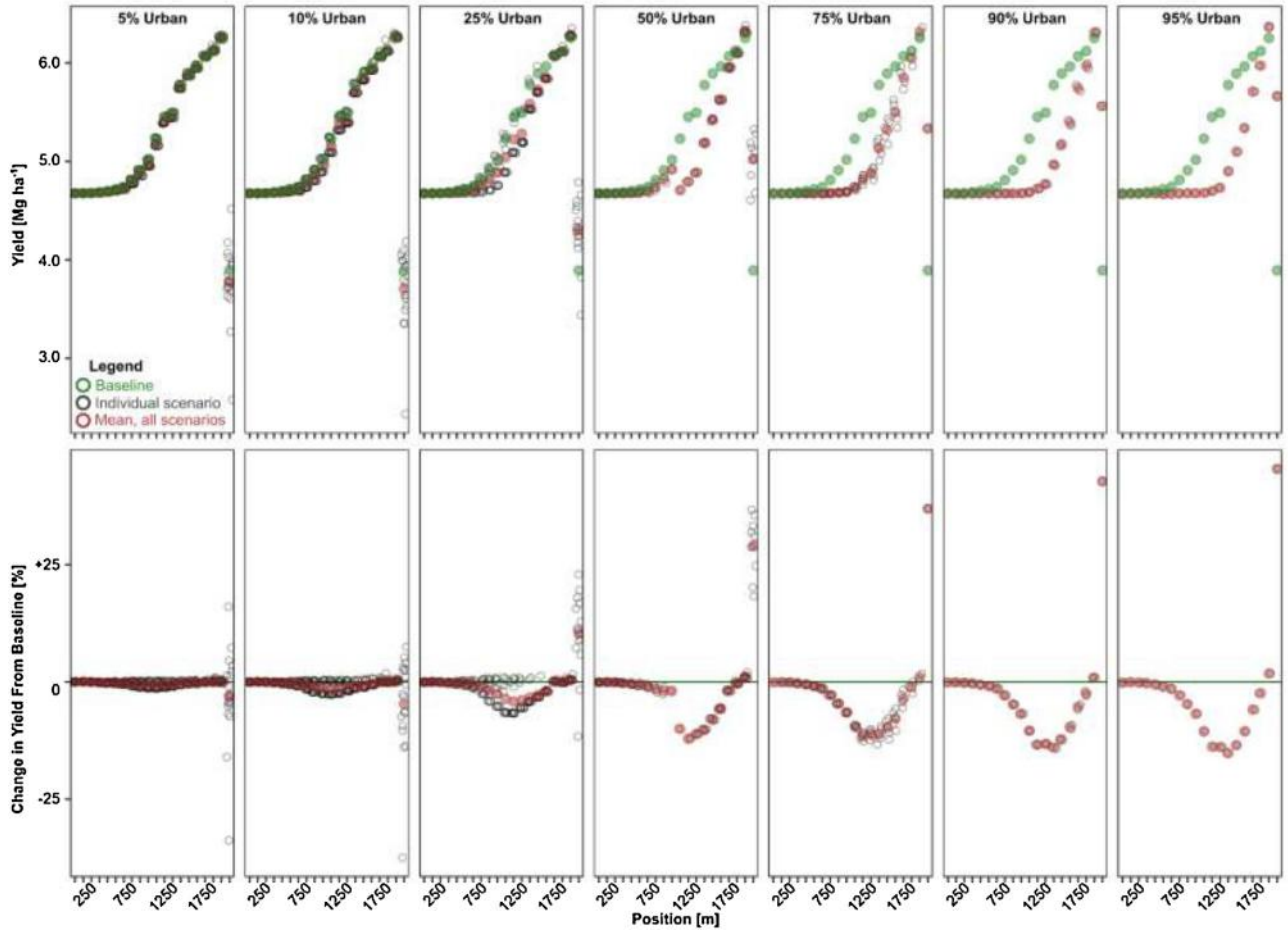

Fig. A4. Yield (top row) and change in yield relative to baseline scenario (bottom row) for all locations and scenarios. Note that bottom row, third column is the same as Fig. 8b.

because both simulations were parameterized as homogeneous soil columns (Wierenga et al., 1991). Overall, this validation indicates that MAGI is able to successfully simulate infiltration and percolation through the vadose zone.

References

Abbott, M.B., Bathurst, J.C., Cunge, J.A., O'Connell, P.E., Rasmussen, J., 1986. An introduction to the european hydrological system — systeme hydrologique europeen, SHE, 2: structure of a physically-based, distributed modelling system. J. Hydrol. 87, 61–77, http://dx.doi.org/10.1016/0022-1694(86)90115-0.

Ahlfeld, D.P., Barlow, P.M., Mulligan, A.E., 2005. GWM-a Ground-water Management Process for the U.S. Geological Survey Modular Ground-Water Model (MODFLOW-2000) (USGS Numbered Series No. 2005–1072), Open-File Report.

Amdan, M.L., Aragón, R., Jobbágy, E.G., Volante, J.N., Paruelo, J.M., 2013. Onset of deep drainage and salt mobilization following forest clearing and cultivation in the Chaco plains (Argentina). Water Resour. Res. 49, 6601–6612, http://dx.doi.org/10.1002/wrcr.20516.

Aquanty Inc, 2015. HydroGeoSphere User Manual. Waterloo, Ontario, Canada.

Arden, S., Ma (Cissy), X., Brown, M., 2014. An ecohydrologic model for a shallow groundwater urban environment. Water Sci. Technol. 70, 1789, http://dx.doi.org/10.2166/wst.2014.299.

Ashby, S.F., Falgout, R.D., 1996. A parallel multigrid preconditioned conjugate gradient algorithm for groundwater flow simulations. Nucl. Sci. Eng. 124, 145–159.

Bhaskar, A.S., Welty, C., 2015. Analysis of subsurface storage and streamflow generation in urban watersheds. Water Resour. Res. 51, 1493–1513, http://dx.doi.org/10.1002/2014WR015607.

Bhaskar, A.S., Welty, C., Maxwell, R.M., Miller, A.J., 2015. Untangling the effects of urban development on subsurface storage in Baltimore. Water Resour. Res. 51, 1158–1181, http://dx.doi.org/10.1002/2014WR016039.

Bhaskar, A.S., Jantz, C., Welty, C., Drzyzga, S.A., Miller, A.J., 2016. Coupling of the water cycle with patterns of urban growth in the Baltimore metropolitan region, United States. JAWRA J. Am. Water Resour. Assoc. 52, 1509–1523, http://dx.doi.org/10.1111/1752-1688.12479.

Bixio, A.C., Gambolati, G., Paniconi, C., Putti, M., Shestopalov, V.M., Bublias, V.N., Bohuslavsky, A.S., Kasteltseva, N.B., Rudenko, Y.F., 2002. Modeling groundwater-surface water interactions including effects of morphogenetic depressions in the Chernobyl exclusion zone. Environ. Geol. 42, 162–177, http://dx.doi.org/10.1007/s00254-001-0486-7.

Bondeau, A., Smith, P.C., Zaehle, S., Schaphoff, S., Lucht, W., Cramer, W., Gerten, D., Lotze-Campen, H., Mueller, C., Reichstein, M., Smith, B., 2007. Modelling the role of agriculture for the 20th century global terrestrial carbon balance. Glob. Change Biol. 13, 679–706, http://dx.doi.org/10.1111/j.1365-2486.2006.01305.x.

Booth, E.G., Loheide, S.P., 2010. Effects of evapotranspiration partitioning, plant water stress response and topsoil removal on the soil moisture regime of a floodplain wetland: implications for restoration. Hydrol. Process. 24, 2934–2946, http://dx.doi.org/10.1002/hyp.7707.

Booth, E.G., Loheide, S.P., 2012. Hydroecological model predictions indicate wetter and more diverse soil water regimes and vegetation types following floodplain restoration. J. Geophys. Res. Biogeosci. 117, G02011, http://dx.doi.org/10.1029/2011JG001831.

Booth, E.G., Zipper, S.C., Loheide, S.P., Kucharik, C.J., 2016. Is groundwater recharge always serving us well? Water supply provisioning, crop production, and flood attenuation in conflict in Wisconsin, USA. Ecosyst. Serv. 21 (Part A), 153–165, http://dx.doi.org/10.1016/j.ecoser.2016.08.007.

Butts, M.B., Payne, J.T., Kristensen, M., Madsen, H., 2004. An evaluation of the impact of model structure on hydrological modelling uncertainty for streamflow simulation. J. Hydrol. The Distributed Model Intercomparison Project (DMIP) 298, 242–266, http://dx.doi.org/10.1016/j.jhydrol.2004.03.042.

Camporese, M., Paniconi, C., Putti, M., Orlandini, S., 2010. Surface-subsurface flow modeling with path-based runoff routing, boundary condition-based coupling, and assimilation of multisource observation data. Water Resour. Res. 46, W02512, http://dx.doi.org/10.1029/2008WR007536.

Cardenas, B.M., 2008. The effect of river bend morphology on flow and timescales of surface water–groundwater exchange across pointbars. J. Hydrol. 362, 134–141, http://dx.doi.org/10.1016/j.jhydrol.2008.08.018.

Carsel, R.F., Parrish, R.S., 1988. Developing joint probability-distributions of soil-water retention characteristics. Water Resour. Res. 24, 755–769, http://dx.doi.org/10.1029/WR024i005p00755.
Cho, J., Barone, V.A., Mostaghimi, S., 2009. Simulation of land use impacts on groundwater levels and streamflow in a Virginia watershed. Agric. Water Manag. 96, 1–11, http://dx.doi.org/10.1016/j.agwat.2008.07.005.
Christian, L.N., Banner, J.L., Mack, L.E., 2011. Sr isotopes as tracers of anthropogenic influences on stream water in the Austin Texas, area. Chem. Geol. 282, 84–97, http://dx.doi.org/10.1016/j.chemgeo.2011.01.011.
Clapp, R.B., Hornberger, G.M., 1978. Empirical equations for some soil hydraulic properties. Water Resour. Res. 14, 601–604, http://dx.doi.org/10.1029/WR014i004p00601.
Coe, M.T., Costa, M.H., Howard, E.A., 2008. Simulating the surface waters of the Amazon River basin: impacts of new river geomorphic and flow parameterizations. Hydrol. Process. 22, 2542–2553, http://dx.doi.org/10.1002/hyp.6850.
Coe, M.T., 1998. A linked global model of terrestrial hydrologic processes: simulation of modern rivers, lakes, and wetlands. J. Geophys. Res. Atmos. 103, 8885–8899, http://dx.doi.org/10.1029/98JD00347.
Coe, M.T., 2000. Modeling terrestrial hydrological systems at the continental scale: testing the accuracy of an atmospheric GCM. J. Clim. 13, 686–704, http://dx.doi.org/10.1175/1520-0442(2000)013<0686:MTHSAT>2.0.CO;2.
Collatz, G.J., Ball, J.T., Grivet, C., Berry, J.A., 1991. Physiological and environmental regulation of stomatal conductance, photosynthesis and transpiration: a model that includes a laminar boundary layer. Agric. For. Meteorol. 54, 107–136, http://dx.doi.org/10.1016/0168-1923(91)90002-8.
Condon, L.E., Maxwell, R.M., 2014. Feedbacks between managed irrigation and water availability: diagnosing temporal and spatial patterns using an integrated hydrologic model. Water Resour. Res. 50, 2600–2616, http://dx.doi.org/10.1002/2013WR014868.
Cuadra, S.V., Costa, M.H., Kucharik, C.J., Da Rocha, H.R., Tatsch, J.D., Inman-Bamber, G., Da Rocha, R.P., Leite, C.C., Cabral, O.M.R., 2012. A biophysical model of Sugarcane growth. Glob. Change Biol. Bioenergy 4, 36–48, http://dx.doi.org/10.1111/j.1757-1707.2011.01105.x.
Dai, Y.J., Zeng, X.B., Dickinson, R.E., Baker, I., Bonan, G.B., Bosilovich, M.G., Denning, A.S., Dirmeyer, P.A., Houser, P.R., Niu, G.Y., Oleson, K.W., Schlosser, C.A., Yang, Z.L., 2003. The common land model. Bull. Am. Meteorol. Soc. 84, http://dx.doi.org/10.1175/BAMS-84-8-1013, 1013-+.
de Graaf, I.E.M., Sutanudjaja, E.H., van Beek, L.P.H., Bierkens, M.F.P., 2015. A high-resolution global-scale groundwater model. Hydrol. Earth Syst. Sci. 19, 823–837, http://dx.doi.org/10.5194/hess-19-823-2015.
de Graaf, I.E.M., van Beek, R.L.P.H., Gleeson, T., Moosdorf, N., Schmitz, O., Sutanudjaja, E.H., Bierkens, M.F.P., 2017. "A Global-Scale Two-Layer Transient Groundwater Model: Development and Application to Groundwater Depletion. Adv. Water Resour. 102 (April), 53–67, http://dx.doi.org/10.1016/j.advwatres.2017.01.011.
Dean, J.F., Webb, J.A., Jacobsen, G.E., Chisari, R., Dresel, P.E., 2015. A groundwater recharge perspective on locating tree plantations within low-rainfall catchments to limit water resource losses. Hydrol. Earth Syst. Sci. 19, 1107–1123, http://dx.doi.org/10.5194/hess-19-1107-2015.
Doble, R., Simmons, C., Jolly, I., Walker, G., 2006. Spatial relationships between vegetation cover and irrigation-induced groundwater discharge on a semi-arid floodplain, Australia. J. Hydrol. 329, 75–97, http://dx.doi.org/10.1016/j.jhydrol.2006.02.007.
Donner, S.D., Kucharik, C.J., 2003. Evaluating the impacts of land management and climate variability on crop production and nitrate export across the Upper Mississippi Basin. Glob. Biogeochem. Cycles 17, 1085, http://dx.doi.org/10.1029/2001GB001808.
Donner, S.D., Kucharik, C.J., 2008. Corn-based ethanol production compromises goal of reducing nitrogen export by the Mississippi River. Proc. Natl. Acad. Sci. 105, 4513–4518.
Donner, S.D., Kucharik, C.J., Foley, J.A., 2004. Impact of changing land use practices on nitrate export by the Mississippi River. Glob. Biogeochem. Cycles 18, GB1028, http://dx.doi.org/10.1029/2003GB002093.
Drewniak, B., Song, J., Prell, J., Kotamarthi, V.R., Jacob, R., 2013. Modeling agriculture in the community land model. Geosci. Model Dev. 6, 495–515, http://dx.doi.org/10.5194/gmd-6-495-2013.
Endrizzi, S., Gruber, S., Dall'Amico, M., Rigon, R., 2014. GEOtop 2.0: simulating the combined energy and water balance at and below the land surface accounting for soil freezing, snow cover and terrain effects. Geosci. Model Dev. 7, 2831–2857, http://dx.doi.org/10.5194/gmd-7-2831-2014.
Falke, J.A., Fausch, K.D., Magelky, R., Aldred, A., Durnford, D.S., Riley, L.K., Oad, R., 2011. The role of groundwater pumping and drought in shaping ecological futures for stream fishes in a dryland river basin of the western Great Plains, USA. Ecohydrology 4, 682–697, http://dx.doi.org/10.1002/eco.158.
Fan, Y., Li, H., Miguez-Macho, G., 2013. Global patterns of groundwater table depth. Science 339, 940–943, http://dx.doi.org/10.1126/science.1229881.
Fan, J., Wang, Q., Jones, S.B., Shao, M., 2016. Soil water depletion and recharge under different land cover in China's Loess Plateau. Ecohydrology 9, 396–406, http://dx.doi.org/10.1002/eco.1642.
Fan, Y., 2015. Groundwater in the Earth's critical zone: relevance to large-scale patterns and processes. Water Resour. Res. 51, 3052–3069.
Farquhar, G.D., Caemmerer, S., Berry, von, 1980. A biochemical model of photosynthetic CO2 assimilation in leaves of C3 species. Planta 149, 78–90, http://dx.doi.org/10.1007/bf00386231.
Faulkner, B.R., Renée Brooks, J., Forshay, K.J., Cline, S.P., 2012. Hyporheic flow patterns in relation to large river floodplain attributes. J. Hydrol. 448–449, 161–173, http://dx.doi.org/10.1016/j.jhydrol.2012.04.039.
Feddes, R.A., Bresler, E., Neuman, S.P., 1974. Field test of a modified numerical model for water uptake by root systems. Water Resour. Res. 10, 1199–1206, http://dx.doi.org/10.1029/WR010i006p01199.
Feddes, R.A., Kowalik, P., Kolinska-Malinka, K., Zaradny, H., 1976. Simulation of field water uptake by plants using a soil water dependent root extraction function. J. Hydrol. 31, 13–26, http://dx.doi.org/10.1016/0022-1694(76)90017-2.
Florio, E.L., Mercau, J.L., Jobbágy, E.G., Nosetto, M.D., 2014. Interactive effects of water-table depth, rainfall variation, and sowing date on maize production in the Western Pampas. Agric. Water Manag. 146, 75–83, http://dx.doi.org/10.1016/j.agwat.2014.07.022.
Foley, J.A., Prentice, I.C., Ramankutty, N., Levis, S., Pollard, D., Sitch, S., Haxeltine, A., 1996. An integrated biosphere model of land surface processes, terrestrial carbon balance, and vegetation dynamics. Glob. Biogeochem. Cycles 10, 603–628, http://dx.doi.org/10.1029/96GB02692.
Foley, J.A., Ramankutty, N., Brauman, K.A., Cassidy, E.S., Gerber, J.S., Johnston, M., Mueller, N.D., O'Connell, C., Ray, D.K., West, P.C., Balzer, C., Bennett, E.M., Carpenter, S.R., Hill, J., Monfreda, C., Polasky, S., Rockström, J., Sheehan, J., Siebert, S., Tilman, D., Zaks, D.P.M., 2011. Solutions for a cultivated planet. Nature 478, 337–342, http://dx.doi.org/10.1038/nature10452.
Foley, J.A., 2005. Global consequences of land use. Science 309, 570–574, http://dx.doi.org/10.1126/science.1111772.
Fry, T.J., Maxwell, R., 2017. Evaluation of distributed BMPs in an Urban Watershed–High resolution modeling for Stormwater Management. Hydrol. Process., http://dx.doi.org/10.1002/hyp.11177.
Garcia-Fresca, B., Sharp, J.M., 2005. Hydrogeologic considerations of urban development: urban-induced recharge. Rev. Eng. Geol. 16, 123–136, http://dx.doi.org/10.1130/2005.4016(11).
Gasper, F., Goergen, K., Shrestha, P., Sulis, M., Rihani, J., Geimer, M., Kollet, S., 2014. Implementation and scaling of the fully coupled Terrestrial Systems Modeling Platform (TerrSysMP v1.0) in a massively parallel supercomputing environment–a case study on JUQUEEN (IBM Blue Gene/Q). Geosci. Model Dev. 7, 2531–2543, http://dx.doi.org/10.5194/gmd-7-2531-2014.
George, R.J., Nulsen, R.A., Ferdowsian, R., Raper, G.P., 1999. Interactions between trees and groundwaters in recharge and discharge areas - A survey of Western Australian sites. Agric. Water Manag. 39, 91–113, http://dx.doi.org/10.1016/S0378-3774(98)00073-0.
Ghamarnia, H., Golamian, M., Sepehri, S., Arji, I., 2010. Shallow groundwater use by Safflower (Carthamus tinctorius L.) in a semi-arid region. Irrig. Sci. 29, 147–156, http://dx.doi.org/10.1007/s00271-010-0226-4.
Giménez, R., Mercau, J., Nosetto, M., Páez, R., Jobbágy, E., 2016. The ecohydrological imprint of deforestation in the semiarid Chaco: insights from the last forest remnants of a highly cultivated landscape. Hydrol. Process. 30, 2603–2616, http://dx.doi.org/10.1002/hyp.10901.
Gleeson, T., Befus, K.M., Jasechko, S., Luijendijk, E., Cardenas, M.B., 2016. The global volume and distribution of modern groundwater. Nat. Geosci. 9, 161–167, http://dx.doi.org/10.1038/ngeo2590.
Graves, R.A., Pearson, S.M., Turner, M.G., 2016. Landscape patterns of bioenergy in a changing climate: implications for crop allocation and land-use competition. Ecol. Appl. 26, 515–529, http://dx.doi.org/10.1890/15-0545.1.
Guo, W., Langevin, C.D., 2002. User's Guide to SEAWAT; a Computer Program for Simulation of Three-Dimensional Variable-Density Ground-Water Flow (USGS Numbered Series No. 6-A7), Techniques of Water-Resources Investigations.
Hain, C.R., Crow, W.T., Anderson, M.C., Yilmaz, M.T., 2015. Diagnosing neglected soil moisture source-sink processes via a thermal infrared-based two-source energy balance model. J. Hydrometeorol. 16, 1070–1086, http://dx.doi.org/10.1175/JHM-D-14-0017.1.
Han, M., Zhao, C., Šimůnek, J., Feng, G., 2015. Evaluating the impact of groundwater on cotton growth and root zone water balance using Hydrus-1D coupled with a crop growth model. Agric. Water Manag. 160, 64–75, http://dx.doi.org/10.1016/j.agwat.2015.06.028.
Harbaugh, A.W., 2005. MODFLOW-2005: the U.S. Geological Survey Modular Ground-Water Model–The Ground-Water Flow Process (USGS Numbered Series No. 6-A16), Techniques and Methods. U.S. Geological Survey.
Harding, K.J., Twine, T.E., VanLoocke, A., Bagley, J.E., Hill, J., 2016. Impacts of second-generation biofuel feedstock production in the central U.S. on the hydrologic cycle and global warming mitigation potential. Geophys. Res. Lett. 43, GL069981, http://dx.doi.org/10.1002/2016GL069981.
Hoffmann, J., Leake, S.A., Galloway, D.L., Wilson, A.M., 2003. MODFLOW-2000 Ground-Water Model: User Guide to the Subsidence and Aquifer-System Compaction (SUB) Package (USGS Numbered Series No. 2003–233), Open-File Report. U.S. Geological Survey.
Homer, C., Dewitz, J., Yang, L., Jin, S., Danielson, P., Xian, G., Coulston, J., Herold, N., Wickham, J., Megown, K., 2015. Completion of the 2011 National Land Cover Database for the conterminous United States - Representing a decade of land cover change information. Photogramm. Eng. Remote Sens. 81, 345–354, http://dx.doi.org/10.14358/PERS.81.5.345.
Hornberger, G.Z., Konikow, L.F., Harte, P.T., 2002. Simulating Solute Transport Across Horizontal-Flow Barriers Using the MODFLOW Ground-Water Transport Process (USGS Numbered Series No. 2002–52), Open-File Report. U.S. Geological Survey.
Houspanossian, J., Kuppel, S., Nosetto, M., Bella, C.D., Oricchio, P., Barrucand, M., Rusticucci, M., Jobbágy, E., 2016. Long-lasting floods buffer the thermal regime

of the Pampas. Theor. Appl. Climatol., 1–10, http://dx.doi.org/10.1007/s00704-016-1959-7.
Huo, Z., Feng, S., Dai, X., Zheng, Y., Wang, Y., 2012a. Simulation of hydrology following various volumes of irrigation to soil with different depths to the water table. Soil Use Manag. 28, 229–239, http://dx.doi.org/10.1111/j.1475-2743.2012.00393.x.
Huo, Z., Feng, S., Huang, G., Zheng, Y., Wang, Y., Guo, P., 2012b. Effect of groundwater level depth and irrigation amount on water fluxes at the groundwater table and water use of wheat. Irrig. Drain. 61, 348–356, http://dx.doi.org/10.1002/ird.685.
Ilstedt, U., Bargués Tobella, A., Bazié, H.R., Bayala, J., Verbeeten, E., Nyberg, G., Sanou, J., Benegas, L., Murdiyarso, D., Laudon, H., Sheil, D., Malmer, A., 2016. Intermediate tree cover can maximize groundwater recharge in the seasonally dry tropics. Sci. Rep. 6, 21930, http://dx.doi.org/10.1038/srep21930.
Jackson, R.B., Canadell, J., Ehleringer, J.R., Mooney, H.A., Sala, O.E., Schulze, E.D., 1996. A global analysis of root distributions for terrestrial biomes. Oecologia 108, 389–411, http://dx.doi.org/10.1007/BF00333714.
Jones, J.W., Hoogenboom, G., Porter, C.H., Boote, K.J., Batchelor, W.D., Hunt, L.A., Wilkens, P.W., Singh, U., Gijsman, A.J., Ritchie, J.T., 2003. The DSSAT cropping system model. Eur. J. Agron. Modell. Cropp. Syst.: Sci. Softw. Appl. 18, 235–265, http://dx.doi.org/10.1016/S1161-0301(02)00107-7.
Karimi, G.H., Naseri, A.A., Behzad, M., Meskarbashi, M., 2011. Groundwater contribution with different salinities on providing maize water requirement and its effects on maize yields. Res. Crops 12, 848–856.
Kim, J.H., Jackson, R.B., 2012. A global analysis of groundwater recharge for vegetation, climate, and soils. Vadose Zone J. 11, http://dx.doi.org/10.2136/vzj2011.0021ra.
Kollet, S.J., Maxwell, R.M., 2006. Integrated surface–groundwater flow modeling: a free-surface overland flow boundary condition in a parallel groundwater flow model. Adv. Water Resour. 29, 945–958, http://dx.doi.org/10.1016/j.advwatres.2005.08.006.
Kollet, S.J., Maxwell, R.M., 2008. Capturing the influence of groundwater dynamics on land surface processes using an integrated, distributed watershed model. Water Resour. Res. 44, W02402, http://dx.doi.org/10.1029/2007wr006004.
Kollet, S., Sulis, M., Maxwell, R.M., Paniconi, C., Putti, M., Bertoldi, G., Coon, E.T., Cordano, E., Endrizzi, S., Kikinzon, E., Mouche, E., Mügler, C., Park, Y.-J., Refsgaard, J.C., Stisen, S., Sudicky, E., 2017. The integrated hydrologic model intercomparison project, IH-MIP2: A second set of benchmark results to diagnose integrated hydrology and feedbacks. Water Resour. Res. 53, 867–890, http://dx.doi.org/10.1002/2016WR019191.
Kucharik, C.J., Brye, K.R., 2003. Integrated Blosphere Simulator (IBIS) yield and nitrate loss predictions for Wisconsin maize receiving varied amounts of nitrogen fertilizer. J. Environ. Qual. 32, 247–268.
Kucharik, C.J., Twine, T.E., 2007. Residue, respiration, and residuals: evaluation of a dynamic agroecosystem model using eddy flux measurements and biometric data. Agric. For. Meteorol. 146, 134–158, http://dx.doi.org/10.1016/j.agrformet.2007.05.011.
Kucharik, C.J., Foley, J.A., Delire, C., Fisher, V.A., Coe, M.T., Lenters, J.D., Young-Molling, C., Ramankutty, N., Norman, J.M., Gower, S.T., 2000. Testing the performance of a dynamic global ecosystem model: water balance, carbon balance, and vegetation structure. Glob. Biogeochem. Cycles 14, 795–825, http://dx.doi.org/10.1029/1999GB001138.
Kucharik, C.J., Barford, C.C., El Maayar, M., Wofsy, S.C., Monson, R.K., Baldocchi, D.D., 2006. A multiyear evaluation of a Dynamic Global Vegetation Model at three AmeriFlux forest sites: vegetation structure, phenology, soil temperature, and CO2 and H2O vapor exchange. Ecol. Model. 196, 1–31, http://dx.doi.org/10.1016/j.ecolmodel.2005.11.031.
Kucharik, C.J., VanLoocke, A., Lenters, J.D., Motew, M.M., 2013. Miscanthus establishment and overwintering in the Midwest USA: A regional modeling study of crop residue management on critical minimum soil temperatures. PLoS One 8, e68847, http://dx.doi.org/10.1371/journal.pone.0068847.
Kucharik, C.J., 2003. Evaluation of a process-based agro-ecosystem model (Agro-IBIS) across the US Corn Belt: simulations of the interannual variability in maize yield. Earth Interact. 7, 14.
Kuppel, S., Houspanossian, J., Nosetto, M.D., Jobbágy, E.G., 2015. What does it take to flood the Pampas?: Lessons from a decade of strong hydrological fluctuations. Water Resour. Res. 51, 2937–2950, http://dx.doi.org/10.1002/2015WR016966.
Lam, A., Karssenberg, D., van den Hurk, B.J.J.M., Bierkens, M.F.P., 2011. Spatial and temporal connections in groundwater contribution to evaporation. Hydrol. Earth Syst. Sci. 15, 2621–2630, http://dx.doi.org/10.5194/hess-15-2621-2011.
Lenters, J.D., Coe, M.T., Foley, J.A., 2000. Surface water balance of the continental United States, 1963–1995: Regional evaluation of a terrestrial biosphere model and the NCEP/NCAR reanalysis. J. Geophys. Res. Atmospheres 105, 22393–22425, http://dx.doi.org/10.1029/2000JD900277.
Liu, Z., Chen, H., Huo, Z., Wang, F., Shock, C.C., 2016. Analysis of the contribution of groundwater to evapotranspiration in an arid irrigation district with shallow water table. Agric. Water Manag. 171, 131–141, http://dx.doi.org/10.1016/j.agwat.2016.04.002.
Lowry, C.S., Loheide, S.P., 2010. Groundwater-dependent vegetation: Quantifying the groundwater subsidy. Water Resour. Res. 46, W06202, http://dx.doi.org/10.1029/2009WR008874.
Lowry, C.S., Loheide, S.P., Moore, C.E., Lundquist, J.D., 2011. Groundwater controls on vegetation composition and patterning in mountain meadows. Water Resour. Res. 47, W00J11, http://dx.doi.org/10.1029/2010wr010086.
Luo, Y., Sophocleous, M., 2010. Seasonal groundwater contribution to crop-water use assessed with lysimeter observations and model simulations. J. Hydrol. 389, 325–335, http://dx.doi.org/10.1016/j.jhydrol.2010.06.011.
Mastrocicco, M., Boz, B., Colombani, N., Carrer, G.M., Bonato, M., Gumiero, B., 2014. Modelling groundwater residence time in a sub-irrigated buffer zone. Ecohydrology 7, 1054–1063, http://dx.doi.org/10.1002/eco.1437.
Maxwell, R.M., Condon, L.E., 2016. Connections between groundwater flow and transpiration partitioning. Science 353, 377–380, http://dx.doi.org/10.1126/science.aaf7891.
Maxwell, R.M., Kollet, S.J., 2008. Interdependence of groundwater dynamics and land-energy feedbacks under climate change. Nat. Geosci. 1, 665–669, http://dx.doi.org/10.1038/ngeo315.
Maxwell, R.M., Miller, N.L., 2005. Development of a coupled land surface and groundwater model. J. Hydrometeorol. 6, 233–247, http://dx.doi.org/10.1175/JHM422.1.
McCown, R.L., Hammer, G.L., Hargreaves, J.N.G., Holzworth, D.P., Freebairn, D.M., 1996. APSIM: a novel software system for model development, model testing and simulation in agricultural systems research. Agric. Syst. 50, 255–271, http://dx.doi.org/10.1016/0308-521X(94)00055-V.
McDonald, M.G., Harbaugh, A.W., 1988. A Modular Three-Dimensional Finite-Difference Ground-Water Flow Model (USGS Numbered Series No. 6-A1), Techniques of Water-Resources Investigations. U.S. Geological Survey.
Merritt, M.L., Konikow, L.F., 2000. Documentation of a Computer Program to Simulate Lake-aquifer Interaction Using the MODFLOW Ground Water Flow Model and the MOC3D Solute-transport Model (USGS Numbered Series No. 2000–4167), Water-Resources Investigations Report. U.S. Geological Survey.
Miguez-Macho, G., Fan, Y., 2012. The role of groundwater in the Amazon water cycle: 2. Influence on seasonal soil moisture and evapotranspiration. J. Geophys. Res. Atmos. 117, D15114, http://dx.doi.org/10.1029/2012jd017540.
Motew, M.M., Kucharik, C.J., 2013. Climate-induced changes in biome distribution NPP, and hydrology in the Upper Midwest U.S.: A case study for potential vegetation. J. Geophys. Res. Biogeosci. 118, 248–264, http://dx.doi.org/10.1002/jgrg.20025.
Motew, M., Chen, X., Booth, E.G., Carpenter, S.R., Pinkas, P., Zipper, S.C., Loheide, S.P., Donner, S.D., Tsuruta, K., Vadas, P.A., Kucharik, C.J., 2017. The influence of legacy P on lake water quality in a midwestern agricultural watershed. Ecosystems, http://dx.doi.org/10.1007/s10021-017-0125-0.
Newcomer, M.E., Gurdak, J.J., Sklar, L.S., Nanus, L., 2014. Urban recharge beneath low impact development and effects of climate variability and change. Water Resour. Res. 50, 1716–1734, http://dx.doi.org/10.1002/2013WR014282.
Niswonger, R.G., Prudic, D.E., 2005. Documentation of the Streamflow-Routing (SFR2) Package to Include Unsaturated Flow Beneath Streams - A Modification to SFR1 (USGS Numbered Series No. 6-A13), Techniques and Methods. U.S. Geological Survey.
Niswonger, R.G., Prudic, D.E., Regan, R.S., 2006. Documentation of the Unsaturated-Zone Flow (UZF1) Package for Modeling Unsaturated Flow Between the Land Surface and the Water Table with MODFLOW-2005 (Techniques and Methods No. 6-A19). U.S. Geological Survey, Reston, VA.
Nosetto, M.D., Jobbagy, E.G., Toth, T., Jackson, R.B., 2008. Regional patterns and controls of ecosystem salinization with grassland afforestation along a rainfall gradient. Glob. Biogeochem. Cycles 22, GB2015, http://dx.doi.org/10.1029/2007gb003000.
Nosetto, M.D., Jobbágy, E.G., Jackson, R.B., Sznaider, G.A., 2009. Reciprocal influence of crops and shallow ground water in sandy landscapes of the Inland Pampas. Field Crops Res. 113, 138–148, http://dx.doi.org/10.1016/j.fcr.2009.04.016.
Nosetto, M.D., Jobbágy, E.G., Brizuela, A.B., Jackson, R.B., 2012. The hydrologic consequences of land cover change in central Argentina. Agric. Ecosyst. Environ. 154, 2–11, http://dx.doi.org/10.1016/j.agee.2011.01.008.
Nosetto, M.D., Acosta, A.M., Jayawickreme, D.H., Ballesteros, S.I., Jackson, R.B., Jobbágy, E.G., 2013. Land-use and topography shape soil and groundwater salinity in central Argentina. Agric. Water Manag. 129, 120–129, http://dx.doi.org/10.1016/j.agwat.2013.07.017.
Nosetto, M.D., Paez, R.A., Ballesteros, S.I., Jobbágy, E.G., 2015. Higher water-table levels and flooding risk under grain vs. livestock production systems in the subhumid plains of the Pampas. Agric. Ecosyst. Environ. 206, 60–70, http://dx.doi.org/10.1016/j.agee.2015.03.009.
Oliveira, P.T.S., Leite, M.B., Mattos, T., Nearing, M.A., Scott, R.L., de Oliveira Xavier, R., da Silva Matos, D.M., Wendland, E., 2017. Groundwater recharge decrease with increased vegetation density in the Brazilian cerrado. Ecohydrology 10, e1759, http://dx.doi.org/10.1002/eco.1759.
Painter, S.L., Coon, E.T., Atchley, A.L., Berndt, M., Garimella, R., Moulton, J.D., Svyatskiy, D., Wilson, C.J., 2016. Integrated surface/subsurface permafrost thermal hydrology: model formulation and proof-of-concept simulations. Water Resour. Res. 52, 6062–6077, http://dx.doi.org/10.1002/2015WR018427.
Passarello, M.C., Sharp, J.M., Pierce, S.A., 2012. Estimating urban-induced artificial recharge: a case study for Austin, TX. Environ. Eng. Geosci. 18, 25–36, http://dx.doi.org/10.2113/gseegeosci.18.1.25.
Pollard, D., Thompson, S.L., 1995. Use of a land-surface-transfer scheme (LSX) in a global climate model: the response to doubling stomatal resistance. Glob. Planet. Change 10, 129–161, http://dx.doi.org/10.1016/0921-8181(94)00023-7.
Prudic, D.E., Konikow, L.F., Banta, E.R., 2004. A New Streamflow-Routing (SFR1) Package to Simulate Stream-Aquifer Interaction with MODFLOW-2000 (USGS Numbered Series No. 2004–1042), Open-File Report. U.S. Geological Survey.
Qiu, J., Turner, M.G., 2013. Spatial interactions among ecosystem services in an urbanizing agricultural watershed. Proc. Natl. Acad. Sci., http://dx.doi.org/10.1073/pnas.1310539110.

Qiu, J., Turner, M.G., 2015. Importance of landscape heterogeneity in sustaining hydrologic ecosystem services in an agricultural watershed. Ecosphere 6, 1–19, http://dx.doi.org/10.1890/ES15-00312.1.
Richards, L.A., 1931. Capillary conduction of liquids through porous mediums. J. Appl. Phys. 1, 318–333, http://dx.doi.org/10.1063/1.1745010.
Rigon, R., Bertoldi, G., Over, T.M., 2006. GEOtop: a distributed hydrological model with coupled water and energy budgets. J. Hydrometeorol. 7, 371–388, http://dx.doi.org/10.1175/JHM497.1.
Robertson, W.M., Sharp, J.M., 2015. Estimates of net infiltration in arid basins and potential impacts on recharge and solute flux due to land use and vegetation change. J. Hydrol. 522, 211–227, http://dx.doi.org/10.1016/j.jhydrol.2014.11.081.
Sacks, W.J., Kucharik, C.J., 2011. Crop management and phenology trends in the U.S Corn Belt: impacts on yields, evapotranspiration and energy balance. Agric. For. Meteorol. 151, 882–894, http://dx.doi.org/10.1016/j.agrformet.2011.02.010.
Sawyer, A.H., Bayani Cardenas, M., Buttles, J., 2011. Hyporheic exchange due to channel-spanning logs. Water Resour. Res. 47, W08502, http://dx.doi.org/10.1029/2011wr010484.
Scanlon, B.R., Reedy, R.C., Stonestrom, D.A., Prudic, D.E., Dennehy, K.F., 2005. Impact of land use and land cover change on groundwater recharge and quality in the southwestern US. Glob. Change Biol. 11, 1577–1593, http://dx.doi.org/10.1111/j.1365-2486.2005.01026.x.
Schneider, A., Logan, K.E., Kucharik, C.J., 2012. Impacts of urbanization on ecosystem goods and services in the U.S. corn belt. Ecosystems 15, 519–541, http://dx.doi.org/10.1007/s10021-012-9519-1.
Seo, H.S., Šimůnek, J., Poeter, E.P., 2007. Documentation of the HYDRUS Package for MODFLOW-2000, the U.S. Geological Survey Modular Ground-water Model (No. GWMI 2007-01). International Ground Water Modeling Center, Colorado School of Mines Golden.
Shields, C., Tague, C., 2015. Ecohydrology in semiarid urban ecosystems: modeling the relationship between connected impervious area and ecosystem productivity. Water Resour. Res. 51, 302–319, http://dx.doi.org/10.1002/2014WR016108.
Shrestha, P., Sulis, M., Masbou, M., Kollet, S., Simmer, C., 2014. A scale-consistent terrestrial systems modeling platform based on COSMO CLM, and ParFlow. Mon. Weather Rev. 142, 3466–3483, http://dx.doi.org/10.1175/MWR-D-14-00029.1.
Silveira, L., Gamazo, P., Alonso, J., Martínez, L., 2016. Effects of afforestation on groundwater recharge and water budgets in the western region of Uruguay. Hydrol. Process. 30, 3596–3608, http://dx.doi.org/10.1002/hyp.10952.
Singha, K., Loheide, S.P., 2011. Linking physical and numerical modelling in hydrogeology using sand tank experiments and COMSOL Multiphysics. Int. J. Sci. Educ. 33, 547–571, http://dx.doi.org/10.1080/09500693.2010.490570.
Sitch, S., Smith, B., Prentice, I.C., Arneth, A., Bondeau, A., Cramer, W., Kaplan, J.O., Levis, S., Lucht, W., Sykes, M.T., Thonicke, K., Venevsky, S., 2003. Evaluation of ecosystem dynamics, plant geography and terrestrial carbon cycling in the LPJ dynamic global vegetation model. Glob. Change Biol. 9, 161–185, http://dx.doi.org/10.1046/j.1365-2486.2003.00569.x.
Soylu, M.E., Istanbulluoglu, E., Lenters, J.D., Wang, T., 2011. Quantifying the impact of groundwater depth on evapotranspiration in a semi-arid grassland region. Hydrol. Earth Syst. Sci. 15, 787–806, http://dx.doi.org/10.5194/hess-15-787-2011.
Soylu, M.E., Kucharik, C.J., Loheide, S.P., 2014. Influence of groundwater on plant water use and productivity: development of an integrated ecosystem –variably saturated soil water flow model. Agric. For. Meteorol. 189–190, 198–210, http://dx.doi.org/10.1016/j.agrformet.2014.01.019.
Steffen, W., Richardson, K., Rockström, J., Cornell, S.E., Fetzer, I., Bennett, E.M., Biggs, R., Carpenter, S.R., Vries, W., Wit, C.A., Folke, C., Gerten, D., Heinke, J., Mace, G.M., Persson, L.M., Ramanathan, V., Reyers, B., Sörlin, S., 2015. Planetary boundaries: guiding human development on a changing planet. Science 347, 1259855, http://dx.doi.org/10.1126/science.1259855.
Sulis, M., Langensiepen, M., Shrestha, P., Schickling, A., Simmer, C., Kollet, S.J., 2014. Evaluating the influence of plant-Specific physiological parameterizations on the partitioning of land surface energy fluxes. J. Hydrometeorol. 16, 517–533, http://dx.doi.org/10.1175/JHM-D-14-0153.1.
Sutanudjaja, E.H., van Beek, L.P.H., de Jong, S.M., van Geer, F.C., Bierkens, M.F.P., 2011. Large-scale groundwater modeling using global datasets: a test case for the Rhine-Meuse basin. Hydrol. Earth Syst. Sci. 15, 2913–2935, http://dx.doi.org/10.5194/hess-15-2913-2011.
Sutanudjaja, E.H., van Beek, L.P.H., de Jong, S.M., van Geer, F.C., Bierkens, M.F.P., 2014. Calibrating a large-extent high-resolution coupled groundwater-land surface model using soil moisture and discharge data. Water Resour. Res. 50, 687–705, http://dx.doi.org/10.1002/2013WR013807.
Šimůnek, J., Šejna, M., Saito, H., Sakai, M., van Genuchten, M.T., 2013. The HYDRUS-1D Software Package for Simulating the One-Dimensional Movement of Water, Heat, and Multiple Solutes in Variably-Saturated Media, Version 4.17, HYDRUS Software Series 3. Department of Environmental Sciences, University of California Riverside, Riverside, CA, USA.
Talebnejad, R., Sepaskhah, A.R., 2015. Effect of different saline groundwater depths and irrigation water salinities on yield and water use of quinoa in lysimeter. Agric. Water Manag. 148, 177–188, http://dx.doi.org/10.1016/j.agwat.2014.10.005.
Thoms, R.B., Johnson, R.L., Healy, R.W., 2006. User's Guide to the Variably Saturated Flow (VSF) Process for MODFLOW (Techniques and Methods No. 6-A18). U.S. Geological Survey, Reston, VA.
Townsend-Small, A., Pataki, D.E., Liu, H., Li, Z., Wu, Q., Thomas, B., 2013. Increasing summer river discharge in southern California USA, linked to urbanization. Geophys. Res. Lett. 40, 4643–4647, http://dx.doi.org/10.1002/grl.50921.
Turner, B.L., Lambin, E.F., Reenberg, A., 2007. The emergence of land change science for global environmental change and sustainability. Proc. Natl. Acad. Sci. 104, 20666–20671, http://dx.doi.org/10.1073/pnas.0704119104.
Twarakavi, N.K.C., Šimůnek, J., Seo, S., 2008. Evaluating interactions between groundwater and vadose zone using the HYDRUS-based flow package for MODFLOW. Vadose Zone J. 7, 757–768, http://dx.doi.org/10.2136/vzj2007.0082.
Twine, T.E., Kucharik, C.J., 2009. Climate impacts on net primary productivity trends in natural and managed ecosystems of the central and eastern United States. Agric. For. Meteorol. 149, 2143–2161, http://dx.doi.org/10.1016/j.agrformet.2009.05.012.
Twine, T.E., Kucharik, C.J., Foley, J.A., 2004. Effects of land cover change on the energy and water balance of the Mississippi River basin. J. Hydrometeorol. 5, 640–655, http://dx.doi.org/10.1175/1525-7541(2004)005<0640:EOLCCO>2.0.CO;2.
Twine, T.E., Kucharik, C.J., Foley, J.A., 2005. Effects of El Niño–Southern Oscillation on the climate, water balance, and streamflow of the Mississippi River Basin. J. Clim. 18, 4840–4861, http://dx.doi.org/10.1175/JCLI3566.1.
Twine, T.E., Bryant, J.J.T., Richter, K., Bernacchi, C.J., McConnaughay, K.D., Morris, S.J., Leakey, A.D.B., 2013. Impacts of elevated CO2 concentration on the productivity and surface energy budget of the soybean and maize agroecosystem in the Midwest USA. Glob. Change Biol. 19, 2838–2852, http://dx.doi.org/10.1111/gcb.12270.
United States Department of Agriculture, 1986. Urban Hydrology for Small Watersheds (2nd edition) (No. TR-55). Natural Resources Conservation Service, Conservation Engineering Division.
Van Genuchten, M.T., 1980. A closed-form equation for predicting the hydraulic conductivity of unsaturated soils. Soil Sci. Soc. Am. J. 44, 892, http://dx.doi.org/10.2136/sssaj1980.03615995004400050002x.
VanLoocke, A., Bernacchi, C.J., Twine, T.E., 2010. The impacts of Miscanthus x giganteus production on the Midwest US hydrologic cycle. Glob. Change Biol. Bioenergy 2, 180–191, http://dx.doi.org/10.1111/j.1757-1707.2010.01053.x.
VanLoocke, A., Twine, T.E., Zeri, M., Bernacchi, C.J., 2012. A regional comparison of water use efficiency for miscanthus, switchgrass and maize. Agric. For. Meteorol. 164, 82–95, http://dx.doi.org/10.1016/j.agrformet.2012.05.016.
Vano, J.A., Foley, J.A., Kucharik, C.J., Coe, M.T., 2006. Evaluating the seasonal and interannual variations in water balance in northern Wisconsin using a land surface model. J. Geophys. Res.-Biogeosci. 111, G02025, http://dx.doi.org/10.1029/2005JG000112.
Vauclin, M., Khanji, D., Vachaud, G., 1979. Experimental and numerical study of a transient, two-dimensional unsaturated-saturated water table recharge problem. Water Resour. Res. 15, 1089–1101, http://dx.doi.org/10.1029/WR015i005p01089.
Verma, P., Loheide II, S.P., Eamus, D., Daly, E., 2014. Root water compensation sustains transpiration rates in an Australian woodland. Adv. Water Resour. 74, 91–101, http://dx.doi.org/10.1016/j.advwatres.2014.08.013.
Wang, E., Robertson, M.J., Hammer, G.L., Carberry, P.S., Holzworth, D., Meinke, H., Chapman, S.C., Hargreaves, J.N.G., Huth, N.I., McLean, G., 2002. Development of a generic crop model template in the cropping system model APSIM. Eur. J. Agron., Process Simulation and Application of Cropping System Models 18, 121–140, http://dx.doi.org/10.1016/S1161-0301(02)00100-4.
Wang, X., Huo, Z., Feng, S., Guo, P., Guan, H., 2016. Estimating groundwater evapotranspiration from irrigated cropland incorporating root zone soil texture and moisture dynamics. J. Hydrol., http://dx.doi.org/10.1016/j.jhydrol.2016.10.027.
Weber, M.D., Booth, E.G., Loheide, S.P., 2013. Dynamic ice formation in channels as a driver for stream-aquifer interactions. Geophys. Res. Lett. 40, 3408–3412, http://dx.doi.org/10.1002/grl.50620.
Webler, G., Roberti, D.R., Cuadra, S.V., Moreira, V.S., Costa, M.H., 2012. Evaluation of a dynamic agroecosystem model (Agro-IBIS) for soybean in southern Brazil. Earth Interact. 16, 12, http://dx.doi.org/10.1175/2012EI000452.1.
Weill, S., Mouche, E., Patin, J., 2009. A generalized Richards equation for surface/subsurface flow modelling. J. Hydrol. 366, 9–20, http://dx.doi.org/10.1016/j.jhydrol.2008.12.007.
Wierenga, P.J., Hills, R.G., Hudson, D.B., 1991. The Las Cruces trench site: characterization, experimental results, and one-dimensional flow predictions. Water Resour. Res. 27, 2695–2705, http://dx.doi.org/10.1029/91WR01537.
Wu, Y., Liu, T., Paredes, P., Duan, L., Pereira, L.S., 2015. Water use by a groundwater dependent maize in a semi-arid region of Inner Mongolia: evapotranspiration partitioning and capillary rise. Agric. Water Manag. 152, 222–232, http://dx.doi.org/10.1016/j.agwat.2015.01.016.
Xu, H., Twine, T.E., Yang, X., 2014. Evaluating remotely sensed phenological metrics in a dynamic ecosystem model. Remote Sens. 6, 4660–4686, http://dx.doi.org/10.3390/rs6064660.
Yira, Y., Diekkrüger, B., Steup, G., Bossa, A.Y., 2016. Modeling land use change impacts on water resources in a tropical West African catchment (Dano, Burkina Faso). J. Hydrol. 537, 187–199, http://dx.doi.org/10.1016/j.jhydrol.2016.03.052.
Zell, C., Kellner, E., Hubbart, J.A., 2015. Forested and agricultural land use impacts on subsurface floodplain storage capacity using coupled vadose zone-saturated zone modeling. Environ. Earth Sci. 74, 7215–7228, http://dx.doi.org/10.1007/s12665-015-4700-4.

Zheng, C., Hill, M.C., Hsieh, P.A., 2001. MODFLOW-2000, the U.S. Geological Survey Modular Ground-water Model: User Guide to the LMT6 Package, the Linkage with MT3DMS for Multi-species Mass Transport Modeling (USGS Numbered Series No. 2001–82), Open-File Report. U.S. Geological Survey.

Zipper, S.C., Loheide, S.P., 2014. Using evapotranspiration to assess drought sensitivity on a subfield scale with HRMET, a high resolution surface energy balance model. Agric. For. Meteorol. 197, 91–102, http://dx.doi.org/10.1016/j.agrformet.2014.06.009.

Zipper, S.C., Soylu, M.E., Booth, E.G., Loheide, S.P., 2015. Untangling the effects of shallow groundwater and soil texture as drivers of subfield-scale yield variability. Water Resour. Res. 51, 6338–6358, http://dx.doi.org/10.1002/2015WR017522.

Zipper, S.C., Qiu, J., Kucharik, C.J., 2016a. Drought effects on US maize and soybean production: spatiotemporal patterns and historical changes. Environ. Res. Lett. 11, 94021, http://dx.doi.org/10.1088/1748-9326/11/9/094021.

Zipper, S.C., Schatz, J., Singh, A., Kucharik, C.J., Townsend, P.A., Loheide, S.P., 2016b. Urban heat island impacts on plant phenology: intra-urban variability and response to land cover. Environ. Res. Lett. 11, 54023, http://dx.doi.org/10.1088/1748-9326/11/5/054023.

Zipper, S.C., Schatz, J., Kucharik, C.J., Loheide, S.P., 2017. Urban heat island-induced increases in evapotranspirative demand. Geophys. Res. Lett. 44, GL072190, http://dx.doi.org/10.1002/2016GL072190.